Proposal for Run IIb Upgrades

The CDF Collaboration

14 June 2001 (V1.0)

Contents

1 Introduction

During the past year the CDF collaboration has undertaken a review of potential upgrades for extending our program of research with the additional integrated luminosity that will be delivered in Run IIb. In many cases we are able to anticipate from prior experience where upgrades will be necessary in order to ensure that the Run IIa capabilities of CDF are preserved in the face of increasing integrated radiation dosage, increasing instantaneous luminosity and the move from 396 to 132 nsec between collisions. There are also many cases where we must await the (hopefully soon!) steady operation of the detector and analyses of some data before we can fully recognize and assess the extent and relative importance of particular upgrades.

Of all the upgrades considered by CDF for Run IIb, the replacement of the SVXII/L00 has the highest priority. The loss of the inner layers of the silicon tracker due to radiation damage would compromise almost all aspects of the CDF research program. A CDF Run IIb Upgrade Steering Committee has endorsed a plan for a full replacement of SVXII and Layer 00 using single-sided silicon detectors readout by SVX-4 chips with a goal of installing the new detector during a $\sim$ 6 month shutdown in the latter part of 2004. (See `http://ncdf12.fnal.gov/PAC/pac_april_01.html` for the proposal submitted to the PAC in November 2000.)

A CDF Run IIb Upgrade Steering Committee has also reviewed internal proposals of additional upgrades in order to set priorities and understand the feasibility and consistency of the upgrades with the desire to minimize the down time for the experiment. In this document we have collected proposals for the other upgrades that we can reliably anticipate as being either required or highly desirable for Run IIb.

In sections 2 to 9 the proposed upgrades are presented roughly in order of the radial location of the hardware from the beamline at CDF. The level of detail in these proposals varies as should be expected given the fact that the various upgrade strategies are more or less dependent on forthcoming results from Run IIa. Questions from the PAC following the April 2001 meeting on the Central Outer Tracker are addressed in part in Section 2. In section 10 we provide a summary of the estimated costs for the upgrades discussed in sections 2 through 9.

In section 11 we provide a summary of the recommendations of CDF's Run IIb Upgrade Steering committee which will guide the work leading to a Technical Design Report for the Run IIb upgrades. In addition, as per the request of the Fermilab Directorate, we provide a rank order list of the upgrades along with some important caveats.

In order to minimize bulk of this document, it is assumed that the reader is able to refer to the Technical Design Report for a description of the baseline upgrade for CDF II and the L00 and Time-of-Flight upgrades. This material is publically available on the web:

`http://www-cdf.fnal.gov/upgrades/tdr/tdr.html`

`http://www-cdf.fnal.gov/upgrades/upgrades.html`

2 "Projective" COT

2.1 Introduction

As Run II luminosity increases, the inner superlayers of the COT will become less effective due to an increase in occupancy. Although track finding utilizing the outer superlayers will still be possible, the ability to point back into the silicon will be degraded due to low hit usage on the inner superlayers. This effect was significant in the latter stages of Run I.

In this section, we outline a method to reduce the occupancy of the inner superlayers of the COT. This method involves making the COT a more "projective" chamber– in other words, deadening the sense wires of the inner superlayers at large $|z|$ (*i.e.* large $|\eta|$.)

The presentation is outlined as follows: we begin by discussing the relationships between instantaneous luminosity, number of interactions per crossing and chamber occupancy. Following that, we propose a scheme to recover COT tracking efficiency at high luminosity by deadening the sense wires at large-$|z|$. After discussing the implications of this scheme, we present how this modification would be implemented. Finally, we present the current status of our work and plan for future activities.

This project is being pursued by James Kraus, Tony Liss and Kevin Pitts of the University of Illinois and Aseet Mukherjee and Bob Wagner of Fermilab.

2.2 Luminosity

The number of $p\overline{p}$ interactions per crossing depends upon the luminosity per bunch. This is shown in Figure 1. The design for the Run IIa CDF detector was based upon the following conditions:

- $\mathcal{L} = 1 \times 10^{32}\mathrm{cm}^{-2}\mathrm{s}^{-1}$, 396 nsec bunch, $\bar{N} \sim 3$,
- $\mathcal{L} = 2 \times 10^{32}\mathrm{cm}^{-2}\mathrm{s}^{-1}$, 132 nsec bunch, $\bar{N} \sim 2$

with the maximum assumed luminosity to be:

- $\mathcal{L} = 2 \times 10^{32}\mathrm{cm}^{-2}\mathrm{s}^{-1}$, 396 nsec bunch, $\bar{N} \sim 6$,

where $\bar{N}$ is the Poisson-distributed average number of interactions per crossing.

To achieve $15\,\mathrm{fb}^{-1}$ of integrated luminosity in 3 years of running (assume 10^7 seconds of live-time per-year) the **average** instantaneous Tevatron luminosity must be $5 \times 10^{32}\,\mathrm{cm}^{-2}\mathrm{s}^{-1}$ which corresponds to $\bar{N} \sim 11$ with 36 bunches or $\bar{N} \sim 5$ with 108 bunches.

As the number of interactions increases, so does the average occupancy. In the following section, we discuss the effect of occupancy on tracking.

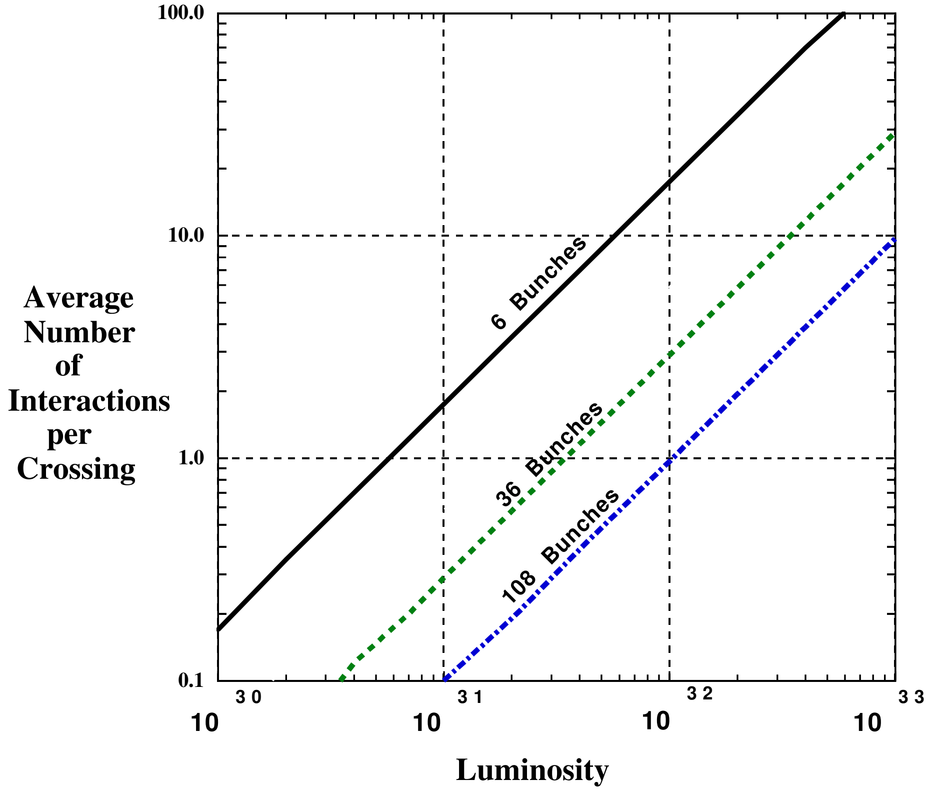

Figure 1: The average number of interactions per crossing as a function of instantaneous luminosity. In 36 bunch running, a luminosity of $\mathcal{L} = 2 \times 10^{32}\,\mathrm{cm}^{-2}\mathrm{s}^{-1}$ corresponds to approximately 6 interactions per crossing.

2.3 Occupancy

Most of the occupancy on the inner superlayers comes from two sources: high-η tracks and "loopers". The loopers are very low-p_T tracks that spiral in the magnetic field. For the COT, tracks from the interaction point with $90 \lesssim p_T \lesssim 130\,\mathrm{MeV/c}$ will pass through part of superlayer 1 and superlayer 2 before spiraling back towards the beamline.

As luminosity increases, the average number of interactions per crossing grows, therefore the average occupancy grows as well. At high luminosity, the occupancy on the inner COT superlayers will be large enough to drastically reduce the effectiveness of those layers. This is shown in Figure 2. For example the CTC hit usage per track at a luminosity of $\mathcal{L} = 2 \times 10^{31}$ was 80% for superlayer 8 and 30% for superlayer 1. For the COT, similar operating conditions will exist at a luminosity of $\mathcal{L} = 1.5 \times 10^{32}\,\mathrm{cm}^{-1}\mathrm{s}^{-2}$ with the Tevatron in 36 bunch mode [1, 2].

Although the Run II silicon system will be more powerful than the Run I silicon, reduced hit usage on inner COT superlayers translates into reduced pointing accuracy. This in turn translates into more ambiguities in associating silicon hits. Also, with a move towards single-sided silicon for the Run IIb system, it is likely that the Run IIb silicon stereo will be weaker than the Run IIa system. If this is indeed the case, then the first stereo superlayer (SL1) of the

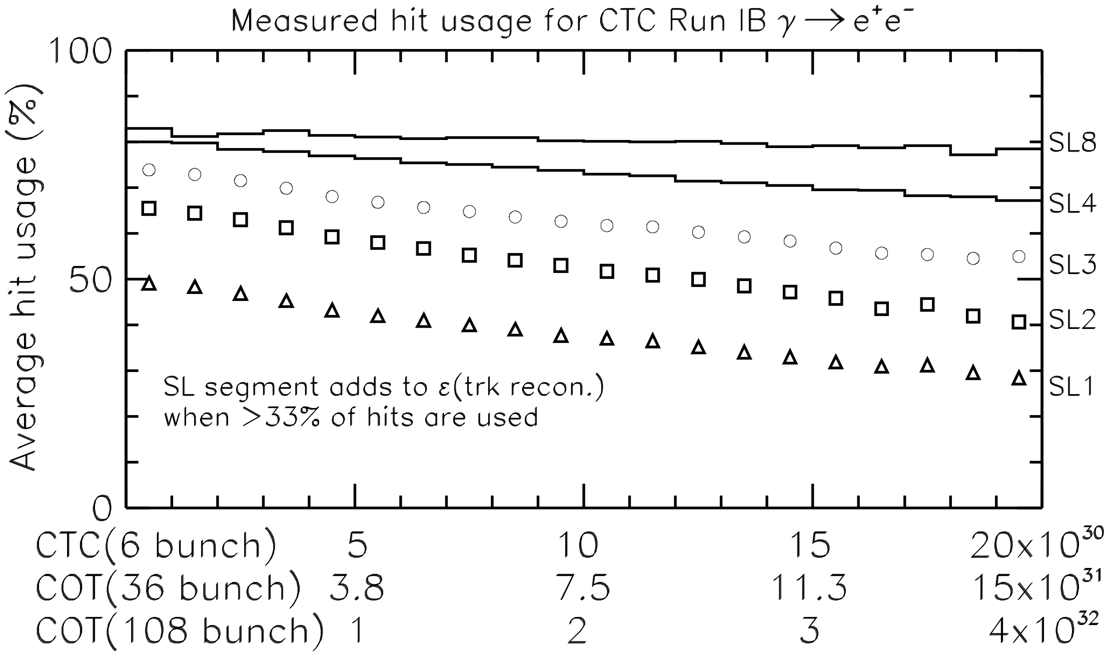

Figure 2: The average hit usage per superlayer as a function of luminosity. These results were measured from Run 1B conversion ($\gamma \rightarrow e^+e^-$) data in the CTC. The hit usage on the inner superlayers (SL1, SL2) is significantly lower than the outer superlayers. In addition, the hit usage on the inner superlayers falls more rapidly than it does for the outer superlayers.

COT will become more significant in the integrated tracking system.

There are a number of ways to discuss wire activity, and the term "occupancy" is used in a number of different ways. In this case, it is not sufficient to discuss "number of hits per wire," because of pulse width effects. The hits caused by high-η tracks and loopers both tend to have larger widths than hits caused by central tracks with $p_T > 400\,\mathrm{MeV/c}$. The hit widths are larger for two reasons:

- Loopers pass through the cell with a very large aspect angle and therefore deposit charge along the entire span of the cell. Although it may show up as one "hit", it renders that wire dead for the entire event.
- High-η tracks deposit more charge due to path length. Even though we will have the dE/dx disabled on the inner superlayers, more charge translates into larger pulse widths.

The figure of merit in this situation is "total time over threshold". Instead of counting hits, we would like to determine what fraction of the time any given wire is alive to see ionization from a central track with $p_T > 400\,\mathrm{MeV/c}$. In the following section, we present a method for improving the response of the inner superlayers at high luminosity by significantly reducing the total time over threshold in those layers.

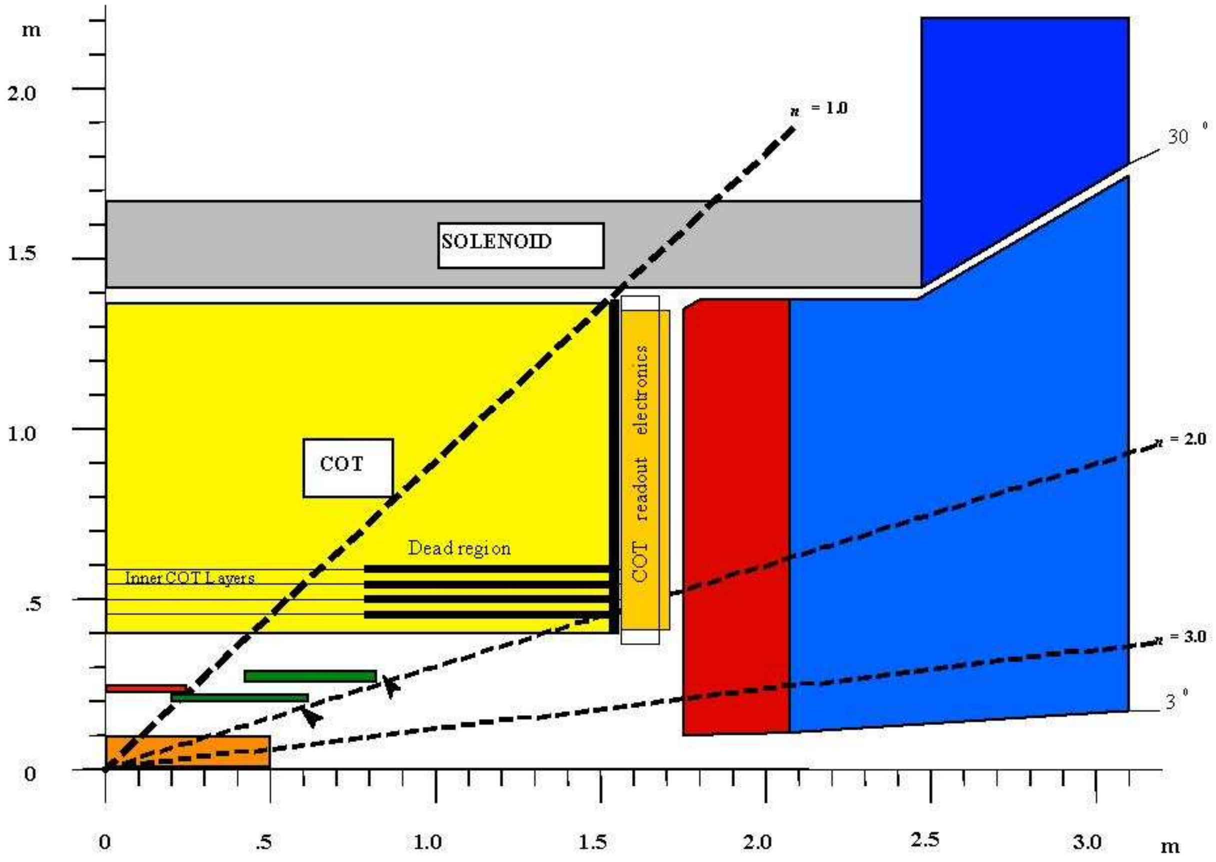

Figure 3: The CDF tracking volume. Superimposed on the COT is a depiction of the profile of the wire-deadening. Although precise dimensions should not be extracted from this picture, the approximate regions are correct for the deadening of superlayer 1 and 2. As is shown from the cartoon, tracks with $|\eta| < 1$ are easily within the active region for all superlayers. Although not clear from the picture, this is true even when a realistic interaction point profile in z is included.

2.4 Wire-deadening

One way to maintain the utility of the inner superlayers is to "deaden" the wires at high $|z|$. In this context, we are using the term "deaden" to signify that the gas gain is lower than it is for the standard sense wires in the COT and primary ionization from a charged track does not translate into a measurable pulse at the preamp. Deadening the wires at high $|z|$ has the advantage of keeping the central part of the chamber alive for tracks with $|\eta| < 1.1$ while removing occupancy from tracks at high $|\eta|$.

The COT is approximately 3 meters long. If we were to render the region with $|z| > 0.75\,\mathrm{m}$ inactive, then the middle 1.5 m would still be active. We would have full efficiency for tracks emanating from $\pm 25\,\mathrm{cm}$ from the interaction point with $|\eta| < 1.1$, while greatly reducing the occupancy from tracks at high-$|\eta|$. The challenge is to have a wire that has normal gain ($\sim 10^4$) from $-0.75\,\mathrm{m} < z < 0.75\,\mathrm{m}$; low (or no) gain for $|z| > 0.75\,\mathrm{m}$; and maintains a conductive path to the chamber endplates for high voltage distribution and signal readout.

In the high luminosity scenario where the inner superlayers are essentially unusable, deadening the wires would reduce occupancy and recover the central region of the COT. The ability to reconstruct high-η tracks would not be "lost", because they could not be reconstructed without wire deadening, either. Figure 4 shows the anticipated COT tracking efficiency (without wire-deadening) as a function of $\cot\theta$. The efficiency falls quite rapidly for $\cot\theta > 1$. A further compromise in efficiency in this region would be a small price to pay in exchange for higher efficiency in the low $\cot\theta$ region in addition to improved SVX linking efficiency. Furthermore, as the luminosity increases the high-η tracking efficiency begins to fall first, because the inner superlayer efficiency is what is lost.

There are a number of ideas for deadening the wires. We won't exhaustively go through all of them here, since this document is simply an expression of interest to begin R&D on this idea. Instead we list two broad classes of possible techniques to deaden the wires:

- Coat the wires with an insulating material. This could be an epoxy or some sort of plastic "jacket" or tube. The issue here is whether or not glow would occur from the Malter effect at the edge of the coating.
- Reduce the drift field (and therefore the gain) by using wires with larger diameter. The wires would be thin in the active region and then become larger in the region we want to deaden. The issues here are how to fabricate wires of this type and concerns that larger (heavier) wires affect the wire sag.

There are a number of advantages to this upgrade path. In the minimal scenario, the only components that would be modified in the entire system would be the superlayer 1 and superlayer 2 wire planes. All other components of the system would be unchanged:

- None of the readout electronics need to be replaced.
- High voltage supplies and distribution are unchanged.

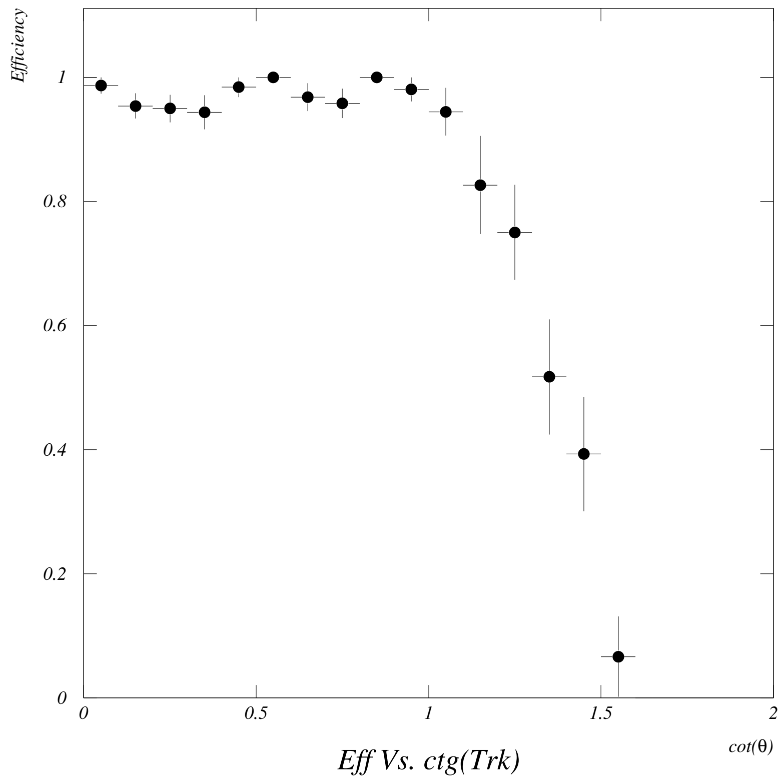

Figure 4: The tracking efficiency as a function of $\cot\theta$ for tracking with the **full** COT (before wire-deadening) [1]. As stated in the text, the efficiency for tracks below $\cot\theta = 1$ would be unaffected by wire-deadening. The efficiency for $1.0 < \cot\theta < 1.5$ would be somewhat compromised.

- The cable plant is unchanged.
- The chamber motherboards and gas seal are unchanged.
- The trigger is unchanged.
- The channel count is unchanged.
- All software is unchanged.

With an upgrade of this type, we would need a period of time to install and test the new sense wire planes, but we would not need to test/debug/commission any new readout electronics. Software would all be 100% compatible before and after this upgrade, although new drift constants would have to be implemented.

As stated in the previous section, the potential for improvement is far greater than a simple reduction in tracks. The larger reduction in total time over threshold will allow the sense wires in the inner superlayers to have a significantly high livetime. We estimate that wire-deadening will reduce the total time over threshold by a factor of 4. We have no direct data to support this claim at this point.

2.5 Construction/Implementation

To implement this plan, we would need to construct new wire planes with modified sense wires. The COT contains 2520 wire planes. This plan calls for the replacement of 360 (14%) of those planes. Experience with the original COT wire-plane construction would be beneficial in this respect.

As noted in the previous section, in this plan the only portion of the COT chamber and readout chain that would need to be modified or replaced would be the wire planes on the inner two superlayers.

The new wire planes would be constructed and tested ahead of time (test fixtures from the COT exist and could be easily resurrected.)

For replacement of the wire planes, the CDF detector would need to be in the assembly area. We are assuming that this replacement would take place during an extended (few month) Tevatron shut-down.

The replacement procedure would be:

- Remove ASD and high-voltage daughterboards.
- Remove ASD and high-voltage motherboards. This step is when the “gas seal” is broken.
- Attach the new wire plane to the old wire plane. The new wire plane is pulled through the chamber as the old wire plane is extracted.

- Test the wire plane, re-install the motherboards, test the wire plane (+ connections) again.
- After all wire planes are installed and tested, remake the gas seal.
- Re-install ASD and high-voltage daughterboards and cables.
- Perform final tests.

We believe that the entire process could be completed in two months with two-shift operations. Recall that the **entire** COT was strung in less than two months. The procedure here is more involved and the environment more difficult.

It should also be noted that the entire procedure poses virtually no threat to the remainder of the chamber.

2.6 A Comment on Aging

During Run 1, the CTC was found to age (loss of gain) at an extremely accelerated rate [3]. A number of studies were performed to understand the cause of this aging. A number of steps have been taken to protect against accelerated aging in the COT. The purpose of this proposal is not to replace the inner sense wires because of accelerated aging. However, it may be in the future that we do have to replace the wire-planes on the inner superlayers. If this were to happen, the procedure outlined in the previous sections would have to take place.

2.7 Status

2.7.1 Electrostatic Calculations

We have performed electrostatic calculations [4, 5, 6] to determine what the wire diameter needs to be to significantly reduce its gain. The results of this study are shown in Figure 5. Recall that our constraints in this case are to have a fully operational and efficient sense wires in the central region of the detector. We therefore choose the standard COT operating point ($40\,\mu$m gold-plated tungsten wire, nominal HV settings) as our baseline. This point is shown in the plot as $d/d_0 = 1$ with a gain of approximately 1×10^4, as expected.

We then vary the wire diameter, keeping all other aspects of the system the same (HV, wire spacing, field sheet orientation) and recalculate the gain. The results show that doubling the wire diameter to $80\,\mu$m reduces the gas gain by a factor of 10 to a gain of 10^3, which effectively deadens the wire.

2.7.2 Simulation Results

We have run the standard CDF Monte Carlo to estimate the performance improvement of the projective COT plan. With the simulation, we compare the effects of having the wires deadened

2000/12/18 14.51

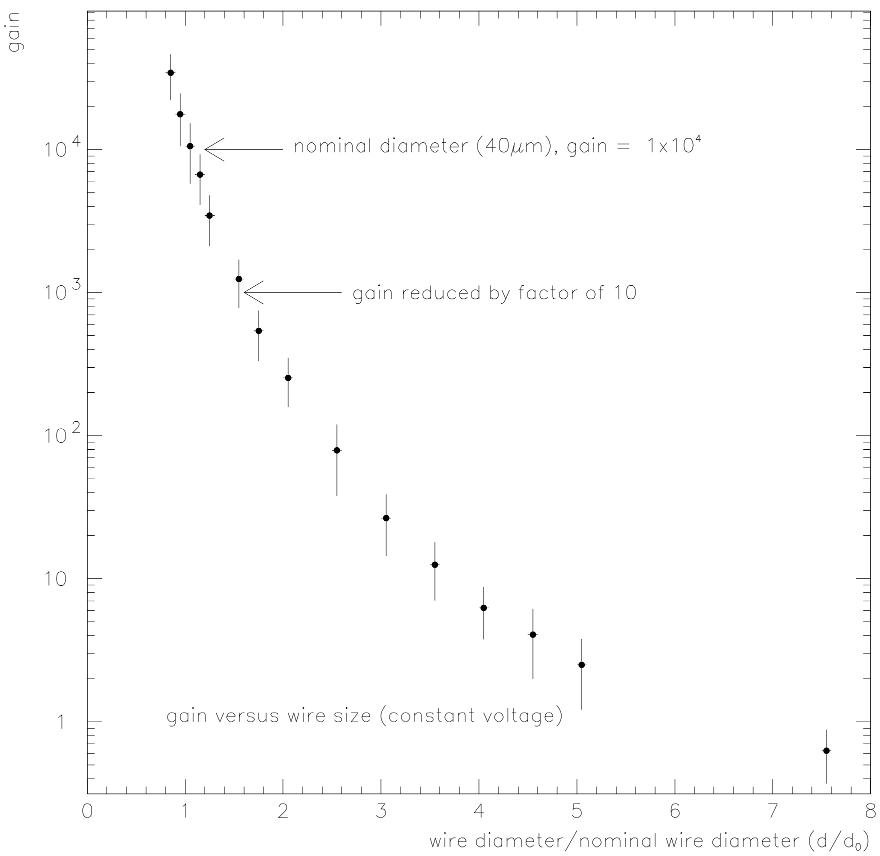

Figure 5: Chamber gain as a function of wire diameter using the nominal COT high-voltage settings. The horizontal axis is the diameter divided by the nominal 40μm diameter used in the COT. The COT operating point is shown at $d/d_0 = 1$ and calculated to have a gain of approximately 10^4, as expected. We find that by doubling the diameter of the sense wire, we can reduce the gain by a factor of 10, thereby effectively deadening the wire.

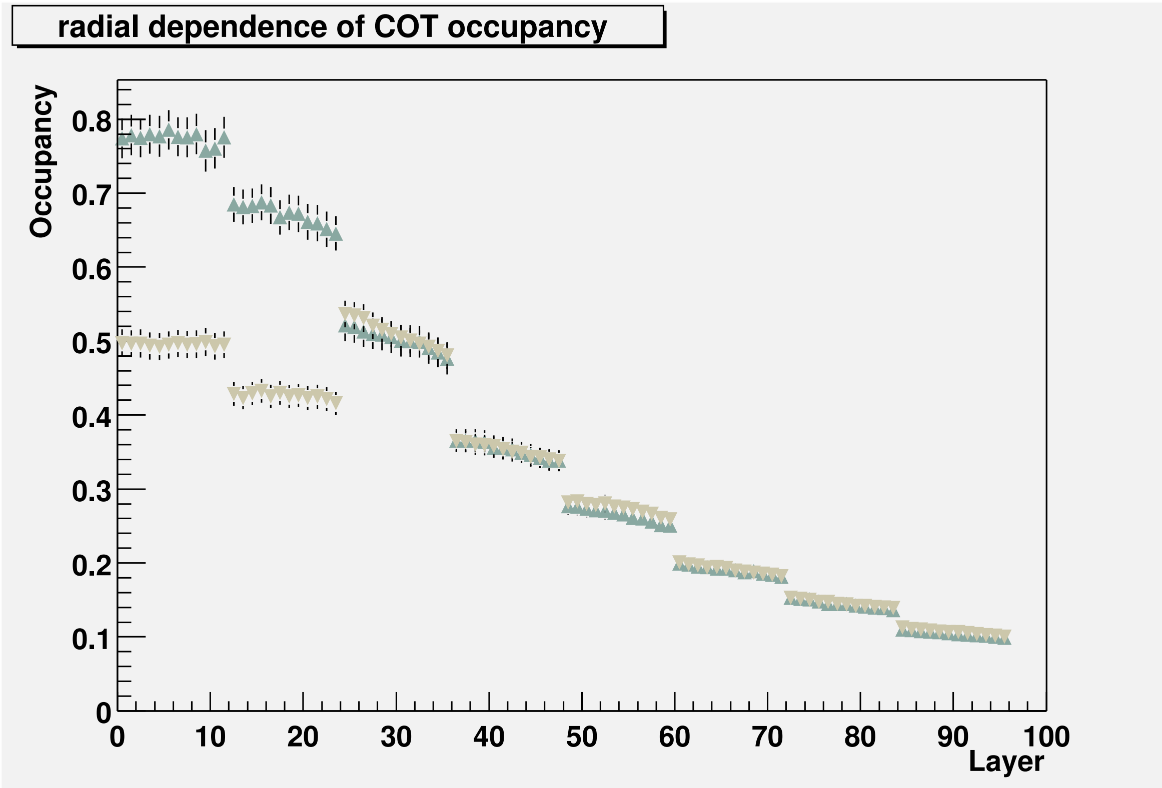

Figure 6: Occupancy as a function of COT layer. Occupancy is defined as the total number of hits divided by the total number of wires. The circles are for the COT, the triangles are for the projective COT. The occupancies are the same for superlayers 3-8 because they are unmodified. The reduction in occupancy is drastic in superlayers 1 and 2.

at high-$|z|$ to the effects of having full-length active wires.

Figure 6 shows the occupancy as a function of layer for a luminosity of $6 \times 10^{32}\,\mathrm{cm}^{-2}\mathrm{s}^{-1}$ with 108 bunches, corresponding to an average of 6 interactions per crossing. The current COT and the projective COT are shown. There are no modifications to superlayers 3-8 (layers 25-96) so the occupancy is identical. The improvement is clearly seen for superlayers 1 and 2, where the occupancy is significantly reduced.

In Figure 6, the occupancy for a given layer is defined as the number of hits per wire divided by the number of wires. This is an underestimate of the improvement in performance for two reasons:

- Hits from loopers have large aspect angle and therefore lead to very large pulse widths, while hits from high-p_T tracks tend to have smaller pulse widths.
- When the occupancy is high, hits from different tracks tend to get merged with one another. Simply counting hits does not account for a reduction in hit-merging.

In fact, for the luminosity shown in Figure 6, the wire occupancy is tending to saturate at SL1. This can be seen in Figure 7, which shows the occupancy as a function of wire-layer (without wire-deadening) for 3, 6 and 9 minimum bias events. On the inner layers, as we go from 6 to 9 minimum bias events, the increase in occupancy is significantly less than it is in going from 3 to 6 minimum bias events. This is because many hits are being added atop existing hits.

Figure 6 shows a 35% reduction in occupancy in the first superlayer (layers 0-11). However, as we argue above, the true occupancy without deadening is significantly underestimated in that figure. As a consequence, the true reduction in occupancy from wire-deadening will be much more than 35%.

We are currently upgrading the simulation so that we may improve our estimates of how well a projective COT will perform. The quantities of interest are the total time over threshold (which is an effective measure of live-time per wire) and the number of good hits found per track.

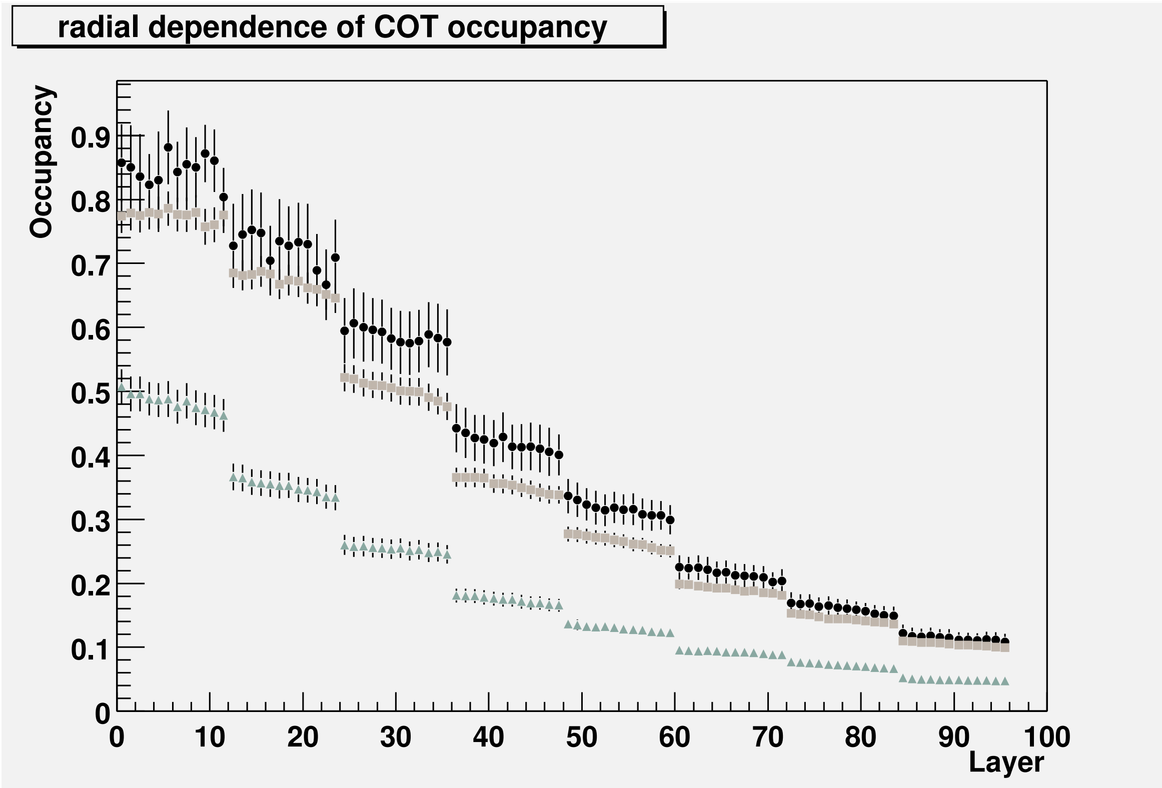

Figure 7: Occupancy as a function of COT layer. Occupancy is defined as the total number of hits divided by the total number of wires. In all cases, the standard COT configuration is shown. The circles are for 9 minimum bias events; the squares are for 6 minimum bias events and the triangles are for 3 minimum bias events. In terms of hit-counting, as is done here, the increase in occupancy in going from 6 to 9 minimum bias events is rather slight because the additional occupancy is piled atop existing hits.

2.8 Plans

Our ongoing plan is threefold.

1. Investigate techniques for deadening the wires. This will involve the construction of a full length, single cell prototype chamber so that we can try out a variety of methods.

2. Continue to perform electrostatic and drift model calculations to understand the requirements and effects of different techniques [4, 5, 6].

3. Use simulation and data to continue to evaluate and optimize the improvement we can achieve by deadening the wires. This will involve understanding chamber response and occupancy contributions as a function of luminosity.

In the meantime, of course, experience will be gained with the COT in the Tevatron environment. This will be a crucial guide to help us understand how to improve COT operation in the future.

2.9 Conclusion

The utility of the COT inner superlayers will begin to degrade at high luminosity. We are expressing an interest in investigating a technique to improve chamber performance at high luminosity by deadening the sense wires at high-$|z|$. This will reject a great deal of unusable "occupancy" while keeping the chamber alive and able to provide data to reconstruct central tracks. In other words, this upgrade would make the COT a projective detector.

References

[1] The CDF-II Collaboration, FERMILAB-Pub-96/390-E (1996).

[2] B. Ashmanskas *et al.*, CDFNOTE 3638 (1996).

[3] B. Wagner *et al.* , CDFNOTE 3175 (1995).

[4] R. Veenhof, GARFIELD Version 6.22, CERN.

[5] W. Riegler *et al.*, CDFNOTE 5050 (1999).

[6] Joel Heinrich, private communication. set up with the Garfield program.

3 Replacement of the Central Preshower Detector and Central Crack Chambers with an Integrated Scintillator Detector (CPR2)

3.1 Introduction

The CDF collabororation proposes to replace the Central Preshower (CPR) and Central Crack (CCR) detectors with an integrated scintillator detector. This would happen at the time the silicon detector is replaced for Run IIb. There are many reasons for this replacement: 1) The CPR is a slow wire chamber that integrates over several crossings and has relatively poor segmentation. This combination will lead to very high occupancies in Run IIb, crippling electron and photon identification. 2) Even with the modest occupancies in Run IIa, the current CPR segmentation makes it difficult to use in more sophisticated analyses such as improving jet resolutions. 3) With 10 fb^{-1} the CPR is expected to have collected 0.1 C/cm, where wire aging has typically caused significant degredation in performance, sometimes beginning with much smaller doses. 4) The thin gas layers of the CPR and CCR have much worse pulse height resolution than a scintillator detector. This is important for both electron identification and improving resolutions with a dead material correction. 5) We have an opportunity to build a much better detector for a relatively small cost, $350-500K. This is possible because we intend to reuse the Run IIa electronics and perhaps use Minos scintillator and other components for the detector.

This project is being pursued by R. Blair[a], C. Bromberg[c],J. Huston[c], S. Kuhlmann[a], R. Miller[c], L. Nodulman[a], A. Rostovtsev[b], and A. B. Wicklund[a] of [a]Argonne National Laboratory, [b]Institute for Theoretical and Experimental Physics (ITEP), and [c]Michigan State University.

3.2 Run I Physics Using the CPR and CCR

There are four potential uses for preshower detectors such as the CPR: 1) improving electron identification, 2) separating single photons from meson backgrounds, 3) improving electron and photon resolutions by correcting for dead material, and 4) estimating the energy deposited in the EM calorimeter by charged hadrons. The CPR has been used extensively in electron identification in CDF. It provides about a factor of two to three more rejection of charged pions that pass all other cuts using tracking, calorimetry, and shower maximum information. This extra rejection has been crucial in soft electron ID for b jet tagging, as was shown in the first top evidence paper and displayed in Figure 8.

Secondly, the CPR has been used in numerous publications involving photon identification. The shower maximum detectors cannot resolve single photons from meson decays above 35 GeV since the angular separation between the two photons is too small. The CPR uses photon conversion rates which are energy independent. It was used initially to extend the QCD measurement of direct photons by more than 100 GeV in photon p_T, as shown in Figure 9. More recently the CPR has been used to estimate backgrounds to signals of exotic physics that include photons. New physics is expected to come at higher p_T, in a region where the shower maximum detector has no discriminatory power. It is crucial to maintain this photon identification capability for possible new signals in Run II. As the next section will show, with the luminosities possible in Run IIb, the occupancy of the current detector will be too large for photon identification.

The third possible use for a preshower detector is to improve electron and photon energy resolutions by correcting for dead material losses. This has not been implemented in CDF to date due to the relatively poor energy resolution of a thin gas detector. The ZEUS experiment has used their scintillator preshower detector to correct for soft photon energy losses in jets, and has seen an improvement in their jet resolution by an impressive 17%[1]. As is well known, improving jet energy resolution will be important in finding various new physics signals such as the Higgs.

Finally, a preshower detector can be used in other ways to improve jet resolutions in algorithms incorporating charged tracking. Since the tracking resolution is so much better than the calorimeter, the main challenge is to estimate the remaining electromagnetic (and neutral hadron) component of the jet. Charged tracks complicate this since they shower in the EM calorimeter, whereas preshower detectors can be used to estimate this contribution to the EM energy. The current CPR detector makes this difficult since a single cell spans five calorimeter towers, possibly collecting showers from other particles in the jet. A preshower detector where each cell is confined to a single calorimeter tower, such as the one in this proposal, is desirable for this purpose.

The current CDF central crack chambers (CCR) have not been directly involved in a CDF publication, but they have been checked for large pulse heights in all of the rare events CDF has observed. Their non-utilization has been due more to a lack of software tools than to their intrinsic usefulness. This has been recently illustrated by a search for a Z peak in dielectron events, where one electron passed into a crack[2]. Figure 10 shows a comparison of the Z peak measured when using the electron + track 4-vector and when one uses the electron + crack energy 4-vector. This indicates the capability of tagging high energy photons in the crack region in events which may contain new physics. The crack covers about 8% of the central detector, and in events with multiple EM objects such as the famous $ee\gamma\gamma Met$ event the possibility of one object hitting the crack is quite high. If we are lucky enough to get a sample of such events then doing measurements of this physics will require crack tagging of photons. Irrespective of the source of this single event, if SUSY is producing signals with photons as some suggest, there will be a large variety of new physics with photons and missing E_T and other objects. Crack tagging of high-energy photons will become even more important. The current crack chamber is a very thin gas layer that would be much improved with a scintillator replacement, integrated with the new preshower detector.

The CDF preshower and crack detectors are expected to play important roles in Run II physics such as soft electron tagging of b jets, photon identification in SUSY events or other new physics, and improving jet resolutions for mass bump searches such as the Higgs. The next section will explain why the CPR in particular will be severely degraded or completely useless in the high-luminosity Run IIb era.

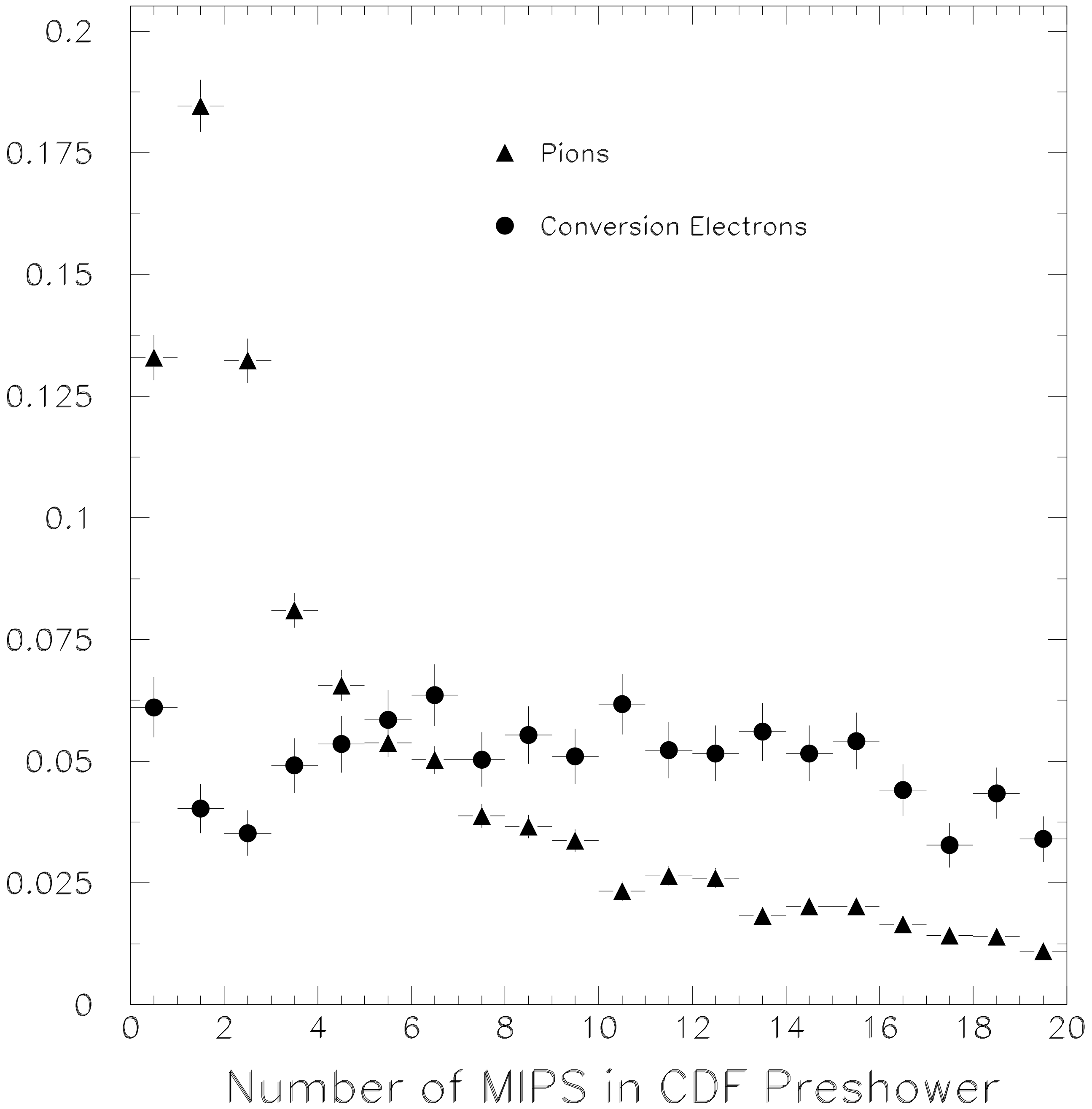

Figure 8: CPR response to electrons and charged pions as shown in the top "evidence" PRD.

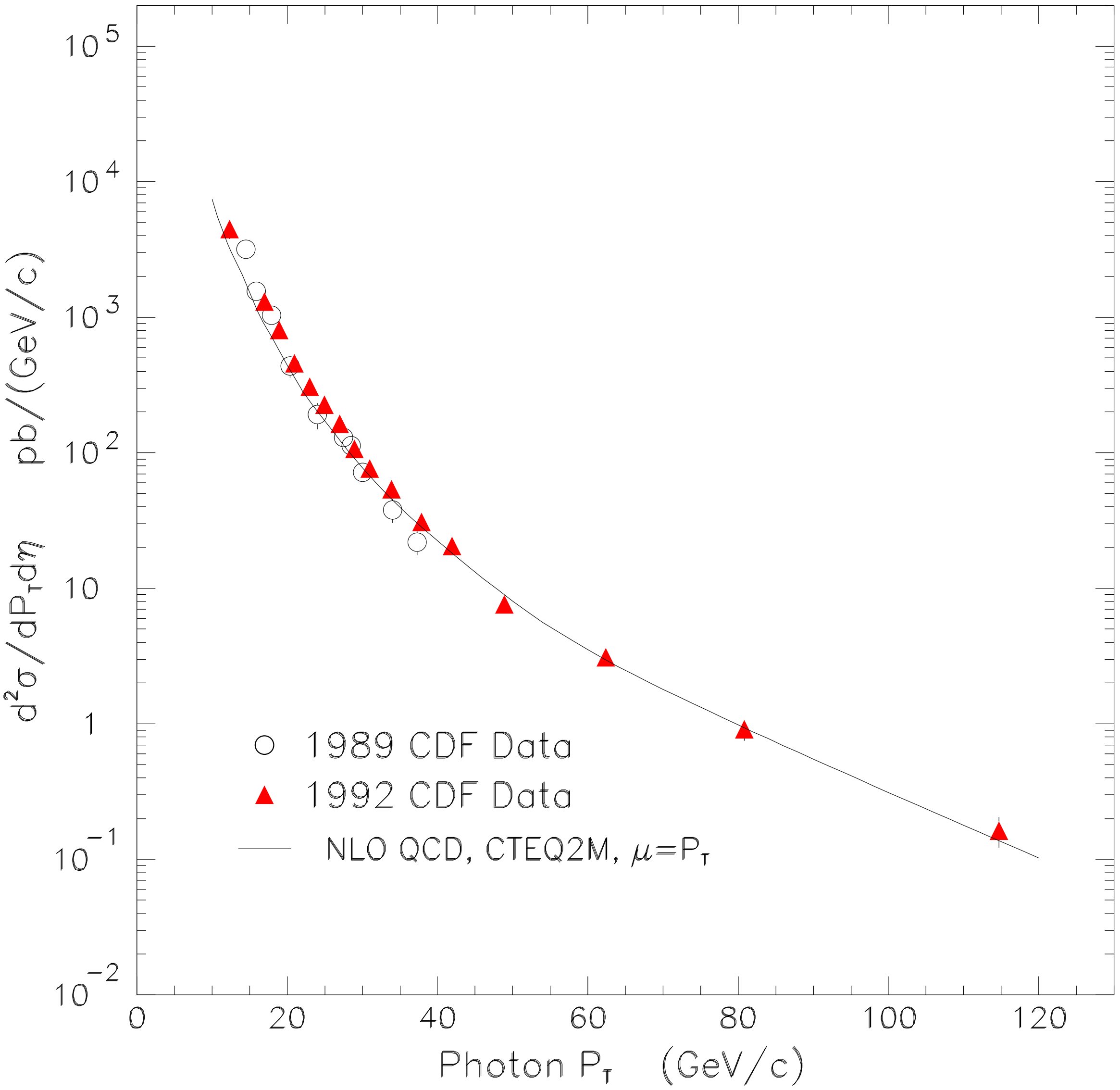

Figure 9: Direct photon cross section from 1989 (before CPR installation) and from 1992 using the CPR. The cross section was extended by almost 100 GeV in photon Pt.

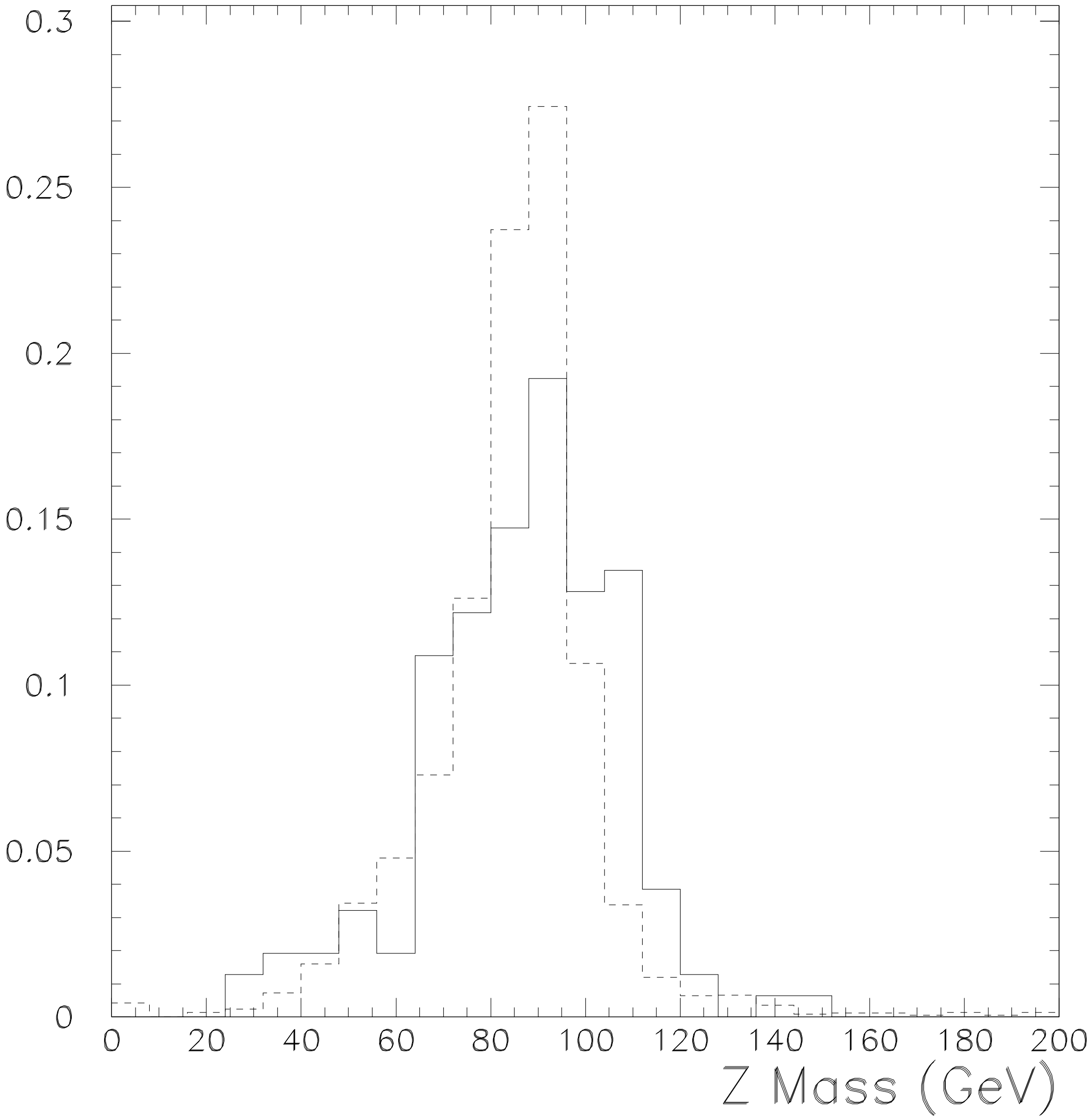

Figure 10: Dashed line is Z peak using electron + track, the solid line is electron plus Crack Chamber pulse height for electrons that went into the ϕ crack.

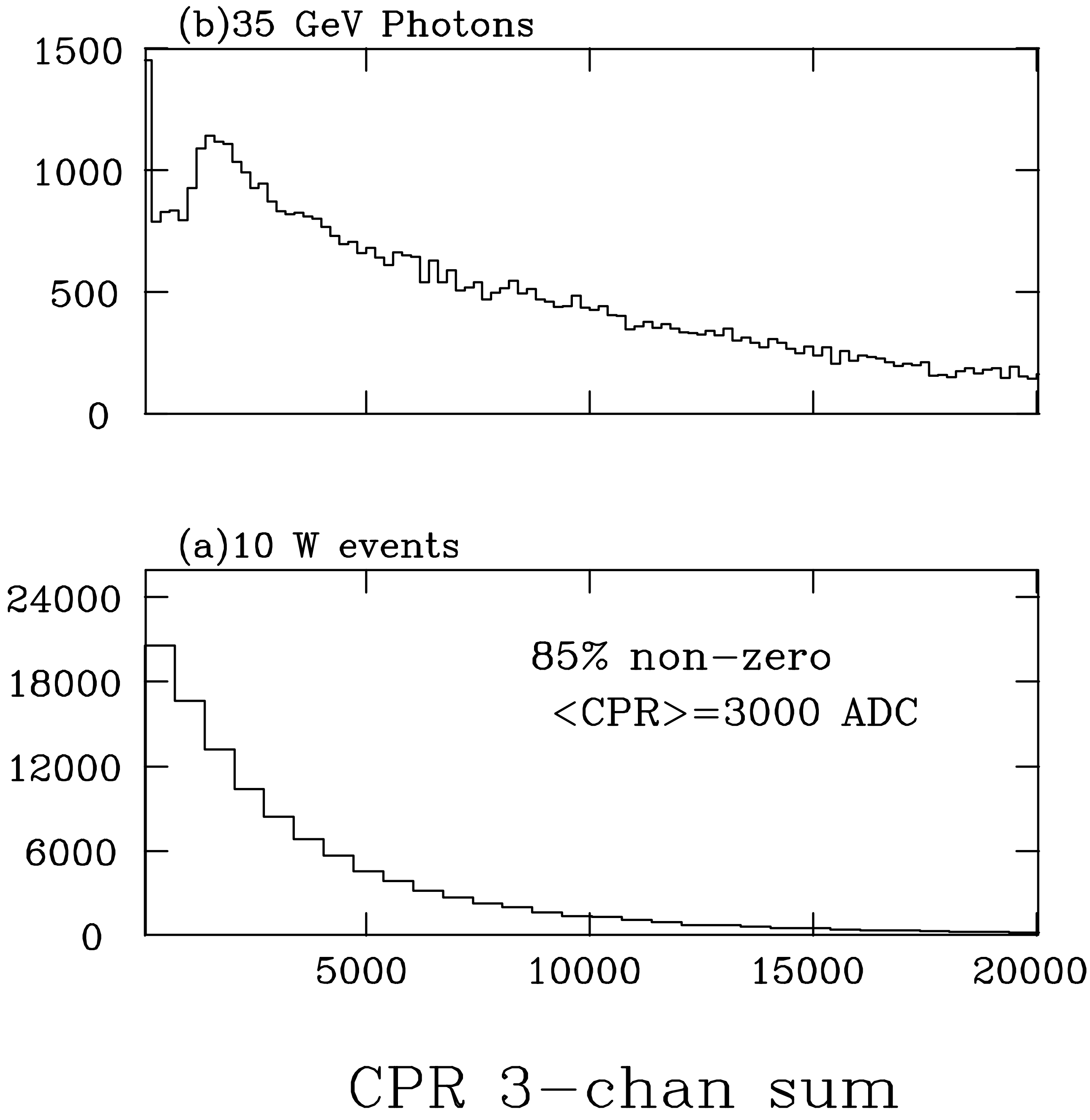

Figure 11: CPR run 1B pulse height distribution for 35 GeV photons (top), compared to an estimated underlying event pulse height distribution at high luminosity. (see text for explanation). The photon cross section is derived from counting the fraction in the zero bin. The 85% occupancy of the estimated underlying event will make this very difficult.

3.3 Occupancy Issues

The occupancy and segmentation issues discussed in this section are only relevant for the preshower detector. The current crack chambers are not sensitive to MIPS or soft photons like the CPR and the proposed crack chambers have the same segmentation as the previous ones. The CPR is a slow wire chamber and, based on early results from the engineering run, it appears that integrating over three or four crossings will be necessary. One concrete example of a problematic scenario is if the peak Run IIb luminosities reach 6x10^{32}, with 108 bunches and 132 ns spacing. This will give rise to 5 minimum bias events per crossing. With the CPR integrating over 4 crossings, the detector will have to deal with over 20 minimum bias events! A second concrete example is the TDR situation of luminosities reaching 2x10^{32}, but with 36 bunches and 396 ns spacing. This results in 6 minimum bias events per crossing. With the CPR integrating over only two crossings in this case, a total of 12 minimum bias events are present in the CPR. With these two examples it is possible to extrapolate to any other possibility. We present Figure 11 as evidence of the serious difficulties the CPR could have in Run IIb. The top plot in Figure 11 shows the run Ib pulse height distribution from photons above 35 GeV. The technique to identify photons at high p_T is to count the fraction of events in the zero bin, since single photons convert less often than multiple photons. In the bottom plot, we took random towers in Run Ib W events (ignoring the electron towers) and overlapped CPR pulse heights from seven of these. Why seven? Since in Run Ib the average number of interactions per crossing was 1.5, this corresponds to 10 minimum bias events. But since W events are more energetic than the typical minimum bias event (by roughly 50%), this situation falls in between the two examples given above. The occupancy of the CPR in this situation is 85%, and there is no discrimination possible between these two plots, rendering the CPR completely useless for photon identification under these conditions. Similar difficulties arise for electron identification. Obviously there is a continuous degradation of performance with increasing luminosities; here we have only mapped out one possibility. But this discussion indicates that the occupancy problems in Run IIb are real.

3.4 Upgraded Detector Design for Run IIb

The relatively limited budget available for the Run IIb upgrades necessitates a limited budget for the CPR upgrade. In this spirit, we plan to re-use the existing electronics channels currently employed in the readout of the existing CPR and CCR detectors, thus removing one of the largest components of the cost for any new detector system. At the time that the present CPR was constructed, the technology did not exist for the convenient design of a scintillator-based device to fulfill the same purpose. In the intervening years, advances in the production of wavelength-shifting (WLS) and clear plastic optical fibers have allowed for the design of scintillator detectors with WLS fiber readout with almost arbitrary segmentation and essentially complete hermeticity. Such a design has already been implemented in CDF in the plug electromagnetic and hadronic calorimeters and in the plug preshower detectors, as well as in many other experiments such as CMS and MINOS.

The new CPR will be placed in the space currently occupied by the old CPR and CCR. The basic design of the new CPR involves scintillator strips, segmented in η and in ϕ, read out by WLS fibers embedded in a groove in one surface of the scintillator. The scintillator for each wedge will be assembled into a mechanical structure ("pizza pan") similar to that used in the endplug calorimeter upgrade. After exiting the strips, the WLS fibers will be routed through grooves in a plastic layer underneath the scintillator to the high eta edge of each wedge, where they will be glued into a number of plastic shell optical connectors. The WLS fibers will be doped with a UV suppressant in order to reduce any cross-talk induced by Cerenkov light as the fibers cross the adjacent towers. The light signals will be routed from these optical connectors through the gap between the central and endwall calorimeters to the back of each wedge of the central calorimeter. There the light signals from each fiber will be coupled to the pixels of the MAPMT's.

Reusing the electronics for CPR/CCR implies two SMD cards per wedge or 64 channels. Note that modification of central SMQIE/SQUID electronics is not required. A possible design would be to retain ten CCR channels and allocate six channels to each of the nine fiducial calorimeter towers. With this segmentation, tower-based information could be used in the optimized jet resolution algorithm. If the six panels per tower were overlapped, one could reach eleven ϕ bins per wedge, but at the expense of a larger occupancy. These tradeoffs of position resolution versus occupancy will be studied early in Run IIa before the CPR2 design is finalized.

Figure 12 (top) shows a possible layout, with no overlapping tiles to reduce occupancy as much as possible. The manner in which the existing MINOS extrusions would be used is indicated. Each segment in $\eta - \phi$ would be read out by 3 WLS fibers. We have maintained the full ten towers in the cracks since the greatest hermeticity possible is mandated for missing energy studies. On the other hand, the tenth tower has never been used in CDF for electron and photon measurements due to poor energy measurement. For this reason we have only instrumented the first nine towers for the preshower section of the detector. The segmentation shown is 2X3 ($\Delta\eta X \Delta\phi$) per calorimeter tower. The bottom figure shows the side view, displaying the embedded fibers and fiber bundles.

3.4.1 Scintillator

The amount of scintillator needed for the new CPR is relatively modest, of the order of 50 m^2. The maximum thickness of the scintillator in the crack region is 0.7 cm due to spacial constraints, while in the rest of the detector the scintillator will be at least 1 cm thick to improve light yield. We are currently exploring several options for the procurement of the scintilator needed, with an eye to optimize both the performance and the cost. The three options are: 1) MINOS scintillator, 2) ITEP Group scintillator, and 3) Bicron scintillator.

MINOS has adopted the technology of (polystyrene-based) scintillator strips read out by WLS fibers for both their near and far detectors. Because of the large volume of scintillator needed, they have chosen the technology of extruding their scintillator into strips of width 4.1 cm and thickness 1 cm with a groove for a 1.2 mm diameter fiber running along one of the large surfaces of the strip. Each strip is coextruded with a TiO2 coating which serves both to

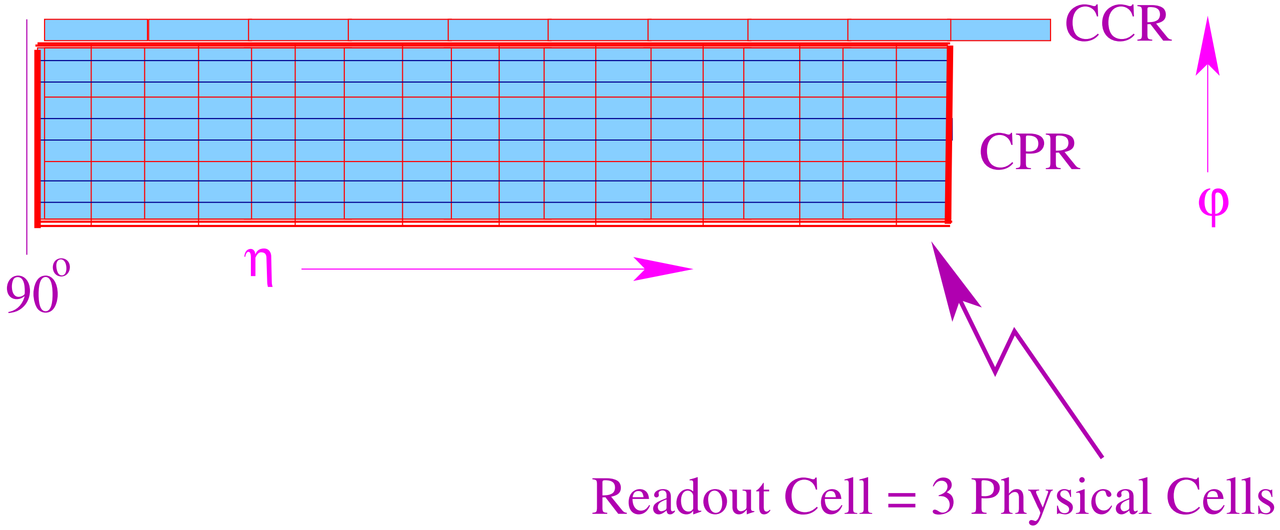

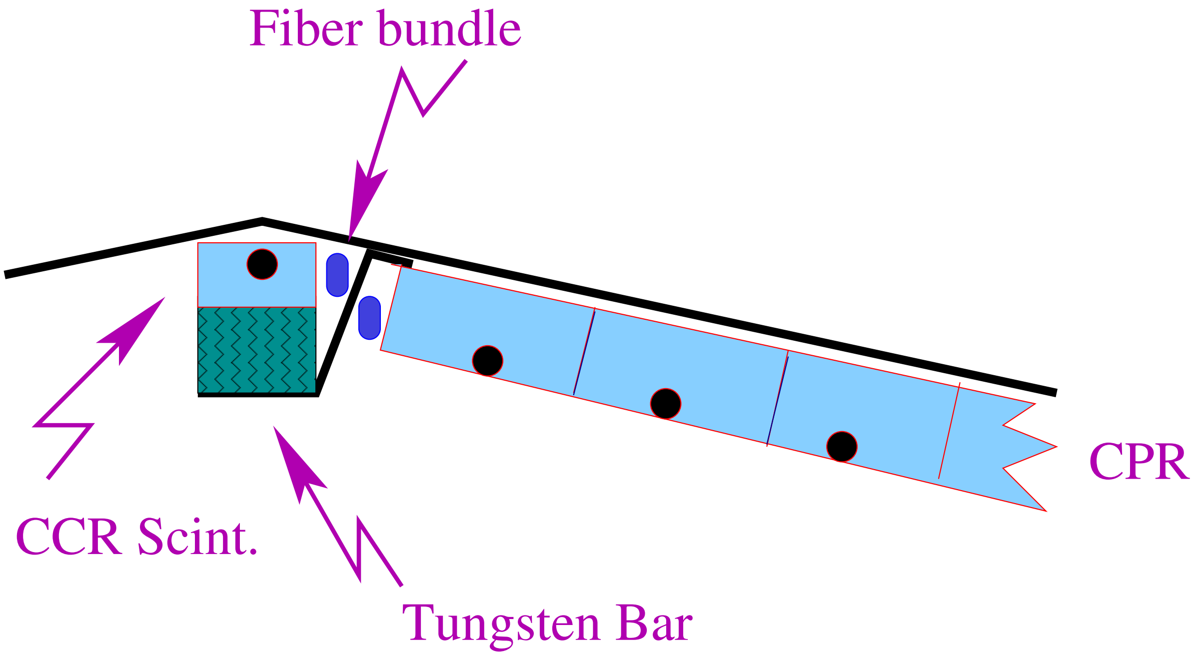

Figure 12: CPR2 layout including crack region. In this design non-overlapping panels (top figure) are used to reduce occupancy. Black circles show the embedded fibers in the bottom figure.

trap the light inside the scintillator as well as allowing for much greater durability and ease of handling. The brightness of the extruded scintillator is comparable to Bicron BC404. MINOS will produce a total of 700,000 m of extruded scintillator of this type. Our requirements will be less than 0.2% of this total. The strip width being used for MINOS may not be optimal for the CPR. A change of extrusion size is easily possible with the production of a new die, at the cost of \$5-10K. If the extrusion width is less than the segmentation size, several WLS fibers from different extrusions in the same readout segment can be coupled to the same MAPMT pixel.

The new CPR will require approximately 500 kg of polystyrene. MINOS is charged a cost of \$2.21 per meter by the extrusion fabrication company. This cost includes the polystyrene pellets, the white capstocking, die and sizing tooling and the purge nitrogen. It is not clear at the moment whether we can obtain the same price as MINOS for our production. Thus, we assume a cost approximately three times larger, given our smaller order. The total extrusion length needed is approximately 1250 m, (assuming the same extrusion width as MINOS) leading to an estimated charge of \$8250. The cost for the scintillating and the WLS dyes needed is approximately (for MINOS) \$0.70/meter. The cost for two extrusion dies (one for the CPR and one for the CCR) is estimated to be \$10K. Thus, we expect a scintillator cost on the order of \$20K from this source. Testing and handling will add another \$20K, leading to a total cost of less than \$40K.

The Russian ITEP group on CDF has the ability to produce 1 cm thick scintillator either by the processes of extrusion or injection molding. The scintillator brightness typically is on the order of 70% of that of Bicron BC404. The cost for production is not currently available but should be cheaper than Bicron.

The third scintillator option is to purchase 1 cm thick scintillator sheets from Bicron of approximate size 0.75 X 2.5 m^2 and then to cut and polish the scintillator strips using the existing facilities in Lab 8. At the same time, a groove for the WLS fiber would be machined. The cost for the scintillator sheets would be approximately \$60K. This option would also require the most handling. This is the most expensive option but is still a relatively small fraction of the total detector cost and is available if the other two options do not work out. The primary choice is the MINOS scintillator extrusion due to its low cost, light yield, durability and ease of handling. As will be discussed later, a prototype is being constructed using this scintillator.

3.4.2 Phototubes

The readout of the detector would be by the use of multi-anode PMT's (MAMPT's). The current choice would be to use the R5900 tube manufactured by Hamamatsu, which is the same tube used for the endplug shower maximum detector. This is a 16 channel device with pixel size of 4.5X4.5 mm^2. With one detector channel per pixel, each wedge of the CPR would require 4 MAPMT's, for a total of 192. If we allow for approximately 5% spares, then the total need would be for approximately 200 MAPMT's. The cost for an order of this size from Hamamatsu is on the order of \$1500/tube, for a total of \$300K. However, MINOS is ordering a large number of these phototubes (on the order of 1500) at a cost of \$700/tube and it may be possible to tie the CDF order into theirs, leading to a cost of the order of \$150K. Several preliminary conversations with the relevant MINOS parties have already taken place regarding this possibility. Each tube will also require a base and mounting at an additional cost of \$100/tube, making the total cost vary between \$170K and \$320K. The lower cost estimate assumes that we can tie our order in with MINOS. We are also exploring the option of using a 64 channel MAPMT produced by Hamamatsu, which has the advantage of leading to only one PMT per wedge. MINOS is also purchasing a large number of the 64 channel MAPMT's, again with a reduced volume discount.

3.4.3 Performance

The new CPR should be sensitive to minimum ionizing particles (MIPS). A yield of 5 photoelectrons per MIP should be sufficient for this purpose. MINOS has achieved a light yield using their standard extrusions of the order of 10 photoelectrons per MIP. This has been achieved through the readout of both ends of the WLS fibers, but also with greater fiber lengths than will be necessary for CDF. The new CPR will read out only one end of the fiber but much of the light transmitted in the other direction will be recovered by mirroring that end of the fiber. The process of depositing an aluminized mirror on a polished fiber end (and then applying a protective coating) was developed for CDF and has become routine in the facility located in the Fermilab village.

The CCR scintillator is forced to be thinner, on the order of 6 mm, than that used for the CPR. This will result in less light but the yield should still be sufficient for the CCR functionality. MINOS uses WLS fibers of diameter 1.2 mm for their detector readout. It may be easiest for the same diameter fibers to be used for the CPR2, but this matter is currently under investigation. Due to its location in the central rapidity region and at a relatively large radius, there should be little impact from radiation damage on the performance of the CPR2, even at the highest forseen luminosities.

3.4.4 R&D/Prototyping

We plan on pursuing a relatively aggressive R&D/prototyping schedule in order to finalize the design parameters. A 4 tower prototype is currently being constructed, making use of scintillator extrusion and wavelength-shifting fiber obtained from MINOS, as well as components left over from the endplug upgrade project. Since each current CPR chamber covers half of a wedge, it will be possible for us to replace a CPR chamber (in the higher η section of a wedge) by our prototype. As discussed previously, tower 9 will not be instrumented. The space will be used to facilitate the optical readout cable routing.

The installation of our prototype detector will enable us to test its performance during the early part of Run IIa. Any 2 week shutdown period in the fall/winter of this year should be sufficient for the prototype installation.

We would like to request \$20K for FY01 and \$30K for FY02 for support of the R&D program work. Most of the money will be directed towards the purchase of materials needed for the prototype. Money can be advanced from the institutions participating in this upgrade in anticipation of a future buy-back.

3.5 Cost Summary

The cost estimate of this detector varies significantly depending on how much we can benefit from the MINOS production lines in both scintillator and phototubes. If both detector and readout can be tied to MINOS the total cost of scintillator + phototubes will be about $190K. In order to tie into the MINOS schedule, the phototubes will need to be ordered by October of 2002. The costs for the WLS and clear optical fibers will depend on the details of the design, but should be in the range of $30-$50K. In addition, design and R&D is $50K, as discussed above. Labor costs for detector construction are estimated to be $120K. For the full readout option, this leads to a total cost of $390-$410K. If neither the detector nor readout can be tied to MINOS then the cost is expected to be closer to $500K.

No foreign sources of funding have been identified as yet, but it may be possible for some labor costs to be contributed by the participating institutions.

3.6 Schedule

R&D/Prototyping/Final Design	Jan 2001 - June 2002
Construction	June 2002 - June 2003
Phototube Procurement	Oct 2002
Phototube Testing	Jan 2003 - Dec 2003
Installation	Run IIb Shutdown

References

[1] S. Magill/ZEUS talk at CALOR2000

[2] CDFNote 4798

4 Addition of Timing Information into the Readout of the Central and Plug Electromagnetic Calorimeters

4.1 Introduction

The CDF Collaboration proposes to add timing information into the readout of the central and plug electromagnetic calorimeters (CEM and PEM) for Run IIb using a technique similar to the hadron TDC (HADTDC) system. This upgrade would significantly improve the potential of the CDF detector to do physics in samples with photons in the final state in two main ways:

1. It would reduce the cosmic ray background sources for important and difficult searches and measurements with final state photons;
2. It would provide a vitally important handle to confirm that all the photons in unusual events, such as the $ee\gamma\gamma\not\!\!E_T$ candidate event [3], are from the primary interaction.

This project (EMTiming) is being pursued by D. Toback, T. Kamon, S.W. Lee, and J. Londoño from Texas A&M University (TAMU), H. Frisch, P. Onyisi and C. Grosso-Pilcher from the University of Chicago, R.G. Wagner from Argonne National Laboratory (ANL), and M. Cordelli from the Laboratori Nazionali di Frascati, Istituto Nazionale di Fisica Nucleare. The effort is being co-led by D. Toback and T. Kamon. We summarize here the full report and supporting documentation which are given in Refs. [1, 2].

Timing information as part of the calorimeter readout has been a part of the CDF detector since it was first commissioned in 1985. The HADTDC system has been a powerful tool to help reject coarse backgrounds from cosmic rays and other non-primary interactions such as beam-gas or main ring splash. Adding timing information to the readout of the CEM and PEM has been suggested periodically over the years as well, but for various reasons it has not been seen as necessary for the primary physics goals of the collaboration.

However, since the observation of the $ee\gamma\gamma\not\!\!E_T$ candidate event and the end of Run I there has been an enormous amount of interest in new models of supersymmetry (SUSY), Higgs decays, and other theories which encourage searches for anomalous events with photons, and in many cases photons and $\not\!\!E_T$. At CDF, there are a number of analyses which either have been or will be submitted to PRL or PRD based on these theories [3, 4]. In each cosmic rays can be an insidious background as they can interact with the detector in various ways which produce an additional photon (and associated $\not\!\!E_T$) which is unrelated to the event. For this reason, it has become apparent that new tools are most needed to reject this background. One such tool which has been used is to look at the time of arrival of the photon relative to the collision time. Such a tool gives us a vitally important handle that confirms that all the photons in unusual events are from a real collision.

4.2 Searching for New Physics with Photons

The primary motivation for doing physics in final states which contain photons is that the photon is likely to be a good probe of new interactions. It is the only one of the three $SU(2) \times U(1)$ gauge bosons that couples to both chiralities (L and R sectors *i.e.*, V vs. V–A or V+A) and is therefore more likely to couple to any new gauge sector. While heavy vector bosons are also likely to couple, the photon has detection advantages over both Ws and Zs as a final state particle. Photons have a better kinematic resolution, and since they do not decay, they do not suffer a sensitivity loss from branching ratios and momentum sharing between the decay products. There are a number of different types of searches for new physics which can be done with photons in the final state.

4.2.1 Electroweak Measurements

Electroweak measurements of diboson production, $W\gamma$ and $Z\gamma$, have been a staple of the community for years and are expected to play a strong role in the Run II physics program. Contamination from cosmic ray backgrounds can occur when a lepton from the primary interaction overlaps with a cosmic ray which gives a photon and $\not\!\!E_T$. In general, the background rate from cosmic ray contamination to diboson events in the charged lepton decay modes is small. However, cosmic rays can cause large disruptions as there is no strong handle on the source of the photon and $\not\!\!E_T$ in the event. For example a $Z \to ee$ event with an overlapping cosmic ray would give an $ee\gamma\not\!\!E_T$ signature. CDF has done a search in inclusive $\ell\gamma\not\!\!E_T$ which is due out shortly [4].

The process $p\overline{p} \to Z^0(\to \nu\bar{\nu}) + \gamma + X$ another excellent example of an analysis that would also be greatly aided by additional cosmic ray background rejection. While this process has the advantage over the $\ell^+\ell^-\gamma$ channel by a factor of 3 in the branching ratio, and almost a factor of 2 in the acceptance, there is as yet no published $\gamma + \not\!\!E_T$ channel measurement of anomalous coupling measurement at CDF. While we can trigger on $\gamma + \not\!\!E_T$ events above 22 GeV, in the current analysis [4] the thresholds must be raised to 55 GeV, where the statistics and sensitivity are greatly diminished, to deal with cosmic ray backgrounds (dominant background by a factor of 7). We hope that with the EMTiming project we could have a highly competitive publication using data in this channel for Run II. We note for completeness that D, which has a pointing calorimeter and has no such problems with cosmic ray backgrounds, has produced the dominant $Z\gamma$ measurement to date by using the $\gamma\not\!\!E_T$ channel [5].

4.2.2 Direct Searches for New Physics with Cosmic Ray Backgrounds

The experimental hints from Run I (for example the $ee\gamma\gamma\not\!\!E_T$ candidate event) and the large number of well-motivated theoretical models help make a compelling case that there are exciting possibilities and prospects for discovery just around the corner for the Fermilab Tevatron. These theories include:

1) Grand Unified Theories which, for example [6], can produce heavy neutrinos which

decay via $\nu_E \rightarrow \gamma n_E$. 2) Composite models of quarks and leptons which, for example [7], produce excited leptons which can decay via $e^* \rightarrow e\gamma$. 3) Models with new dynamics which, for example [8, 9], produce anomalous production of $W\gamma$ and $Z\gamma$ events. 4) Models with large extra dimensions can, for example [10, 11], have the emission of electromagnetic radiation in Gravitino pair production producing events with the $\gamma \not\!\!E_T$ final state signature. 5) In certain Higgs models, there are fermiophobic Higgs bosons [12] which can decay via $H \rightarrow \gamma\gamma$. 6) In recent SUSY models, two main choices of SUSY breaking have come into favor which predict photons in the final state. Supergravity models can, for example [13], produce events which decay down to neutralinos, N_2, such that the decay $N_2 \rightarrow \gamma N_1$ dominates, or $N_1 \rightarrow \gamma \tilde{G}$ [14]. In some gauge-mediated SUSY breaking models (GMSB) [13, 15, 16] all SUSY cascade decays can end in $N_1 \rightarrow \gamma \tilde{G}$, and all events have 2 photons and (some) $\not\!\!E_T$. The SUSY signals are of particular interest, as they provide a natural explanation for the $ee\gamma\gamma\not\!\!E_T$ candidate event.

4.2.3 Quasi-Model-Independent Searches

While there are a large number of theories which predict new particles which decay to photons, with or without $\not\!\!E_T$, a potentially far more powerful motivation is based on the idea that we have not yet have correctly guessed the mechanism of electroweak symmetry breaking. This suggests that there is a good chance that the data will point the way first. Perhaps our best hint of new physics in Run I was the observation of the $ee\gamma\gamma\not\!\!E_T$ candidate event. There are new strong techniques for making these types of exploratory searches both quantitative and systematic and we intend to use them [3, 17]. In Run II, even with twenty times the data, in the case that we do see a statistically significant excess of such events, it is still likely to be at relatively low statistics so we will need all the background rejection we can get. Furthermore, as in the case for the $ee\gamma\gamma\not\!\!E_T$ candidate event, even the most lenient critics will want to see that on a case-by-case basis any unusual events containing photons (and especially those with $\not\!\!E_T$) are not due to cosmic ray sources. In these cases, with no model to guide the experimenter on ways to verify an explanation, timing information is crucial.

4.2.4 Future Possibilities: Long-Lived Particles which Decay to Photons

It is possible that with enough time and calibration data ($W \rightarrow e\nu$) the system would allow for a new class of searches for long-lived particles which decay to photons. In a GMSB scenario where $\tilde{G}$ and N_1 are the LSP and NLSP, the $\tilde{G}$ mass is expected to be in the range between 1 eV/c^2 and 10^4 eV/c^2 [16]. This can lead to an N_1 which can decay via $N_1 \rightarrow \gamma\tilde{G}$ with lifetimes of order (1-10 ns). If we can calibrate the timing to better than 1 nsec, the system should be powerful enough to study this class of models. The current HADTDC system has approximately 5 nsec of timing resolution without any real calibration of the system. These calibration issues are still under study. The issues of how efficiently the photon identification will do with photons which come from a position displaced from the vertex will also have to be studied.

4.3 The EMTiming Project

The proposed EMTiming upgrade is similar to the HADTDC system which records the time of arrival of any energy deposited. In Run I, the HADTDC system was used to find the 'timing' of photons [18]. Even though most of a photon's energy is deposited in the CEM or PEM, there is some leakage into the HAD. Figure 13 shows a comparison of the timing in the HADTDC's for promptly produced particles and for cosmic rays. As shown in the figure prompt particles have a distribution which is centered at the time of flight from the collision point to the calorimeter with a resolution of a few nsec. Cosmic rays are spread evenly as a function of time. Rejection of cosmic ray backgrounds using timing in the calorimeter clearly has excellent rejection power, and allows for a straight forward method of background estimation.

Unfortunately, even though many photons deposit some energy in the HAD, the efficiency of getting timing information is often not high, and more importantly is a strong function of the E_T of the photon. The efficiency is roughly 20% for $E_T^\gamma = 20$ GeV and plateaus around 100% above about 80 GeV. See Figure 14. Such an efficiency is deadly in many standard analyses. For example, in many models of GMSB the photons have mean E_T's of 50 GeV and 30 GeV which would have a mean efficiency of 70% and 35% respectively, for a mean event efficiency of only 25% before any identification or kinematic requirements. The efficiency for the EMTiming project for any photon should easily be 100% and be flat in E_T.

4.3.1 Tell-tale Handles in Important Events

The efficiency loss in using the HADTDC's to do *apriori* photon physics searches is disappointing. However, *a posteriori* this inefficiency could undermine any confidence in a potential discovery. The pressing nature of having a high efficiency timing measurement is illustrated in Figure 13 which also contains the timing for the two electron and two photon candidates in the $ee\gamma\gamma\not\!\!E_T$ event. Only three of the four objects were in the central calorimeter, and only two of the four deposited enough energy in the HAD to fire the TDC's. Even so, the photon was barely above threshold. The fact that both the electron and one photon are in time is actually quite an interesting result as it helps confirm that at least part of the event is from the primary collision. While there are estimates as to the rate at which cosmics can contribute photons to an already existing event (and such estimates appear to be negligible [3]) it is clear that statistics are a worry in a sample of a few events, and an even greater worry in a sample of one event. Direct timing for both the CEM and PEM are, and would have been, of great benefit in this important instance. We will never know if this event was an overlap.

4.4 Hardware, Cost, Schedule and Manpower

The hardware for this system is designed to mimic that of the Hadron TDC system as much as possible. Since there is no new technology in this design, we have not supplied a great deal of technical detail in this summary. More details can be found in Refs. [1, 2]. A summary of the parts, including costs, can be found in Table 1. The path is:

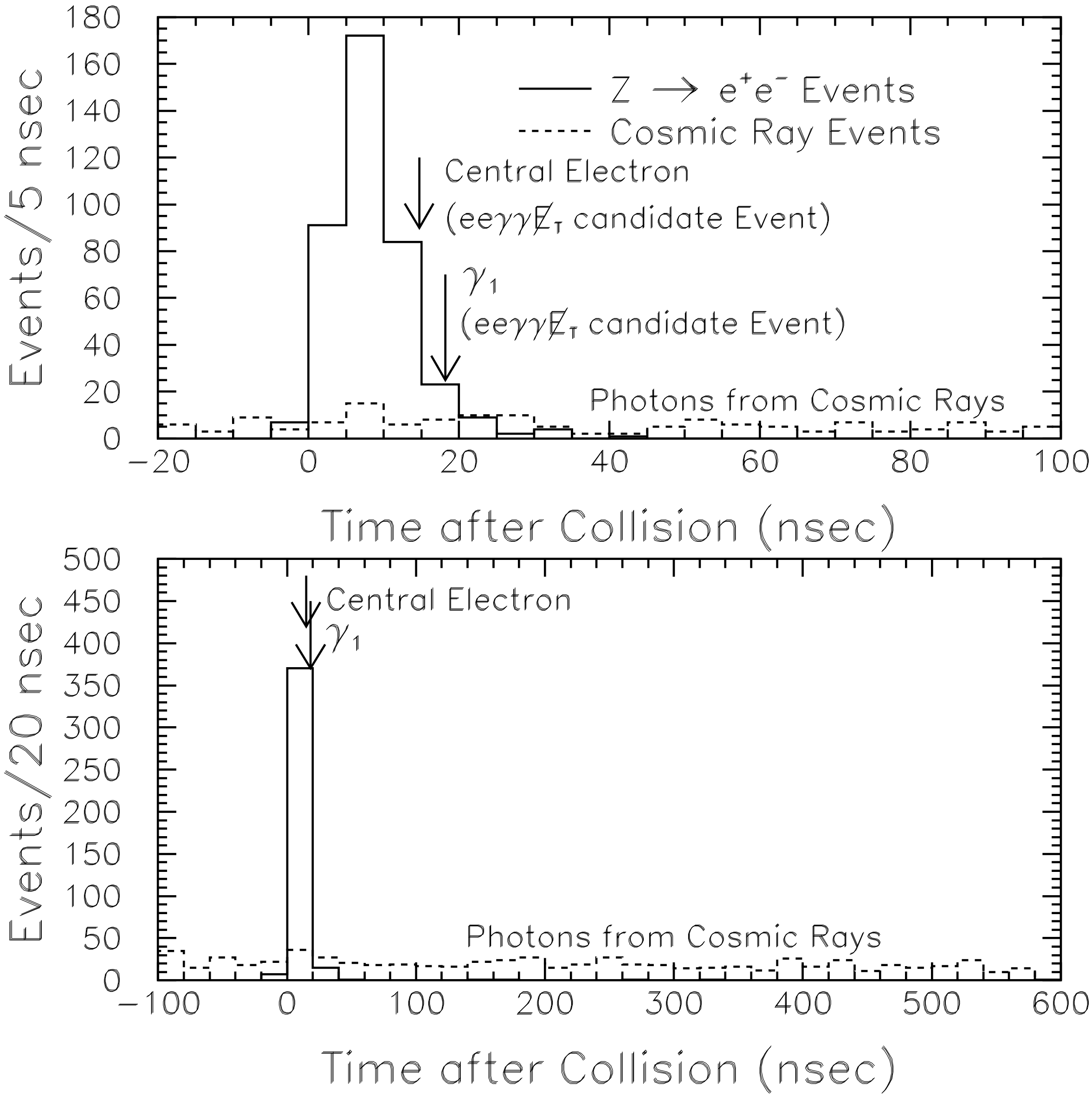

Figure 13: A comparison of the timing information for electrons from $Z \to ee$ and cosmic rays events using the central hadron calorimeter in Run I. Note that for true electrons the distribution is centered at the time of flight from the collision point to the calorimeter and that the unoptimized resolution is a few nsec. Cosmic rays are spread evenly as a function of time as expected. We include the timing of two of the four EM clusters in the CDF $ee\gamma\gamma\not\!\!E_T$ event as only two were in the central part of the calorimeter and deposited enough energy to fire the HADTDC's. We also note that the photon was barely above threshold for timing information.

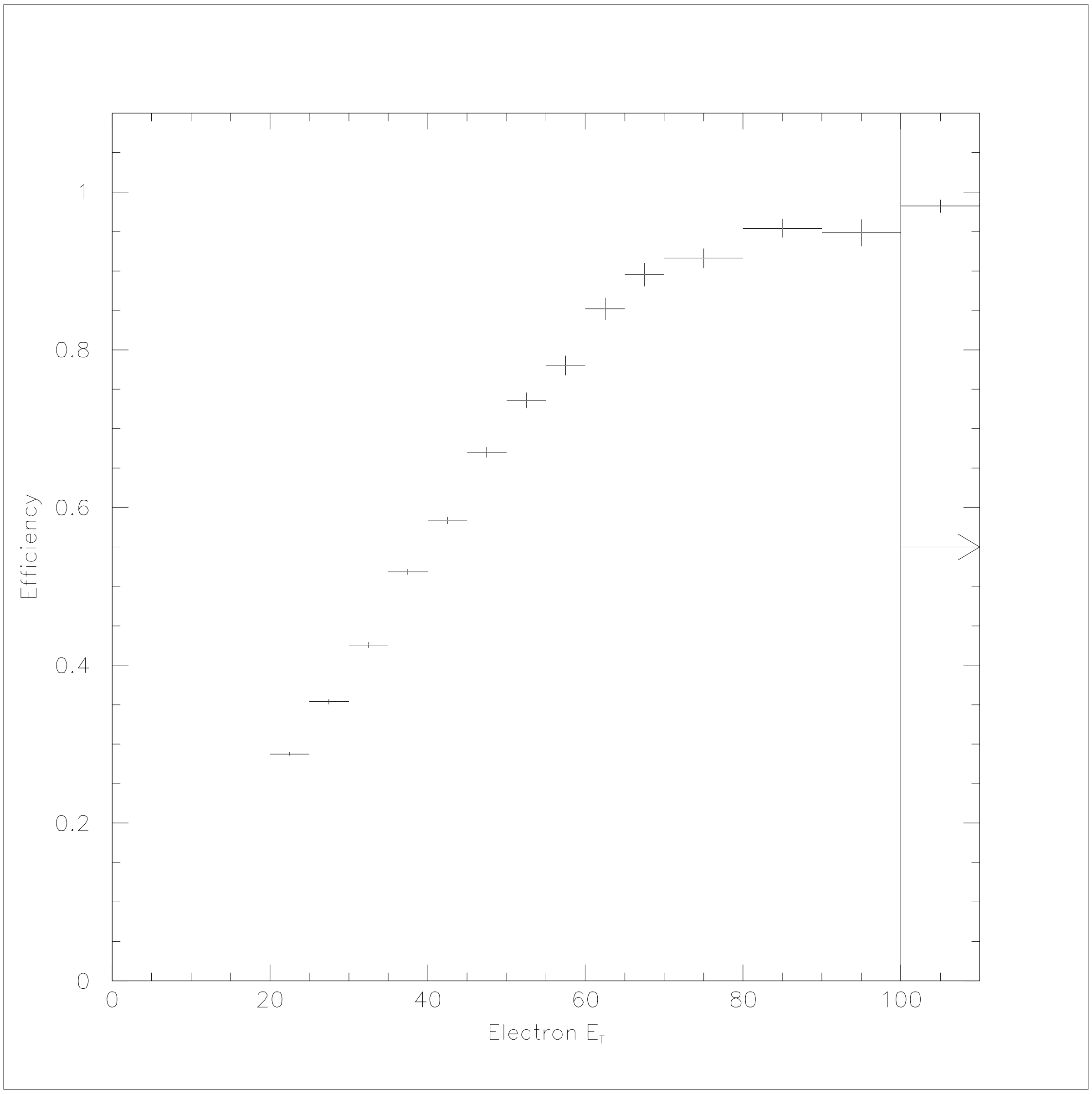

Figure 14: Efficiency for electrons to have enough energy deposited in the hadronic calorimeter to fire the TDC's, and be within the timing window. We assume that the efficiency for electrons and photons are equal since their shower charactaristics are similar for the amount of energy deposition in the HAD. Note that the region to right of line is all events above 100 GeV.

$$\text{PMT/Base} \xrightarrow{\text{Cable}} \text{Transition Card} \xrightarrow{\text{VME Backplane}} \text{ASD} \xrightarrow{\text{Cable}} \text{Patch Panel} \xrightarrow{\text{Cable}} \text{TDC} \xrightarrow{\text{VME}} \text{Readout}$$

Currently there are 960 CEM phototubes, none of which have a base which is compatible with readout for timing. To remedy this we propose adding a dynode line out which requires that all the bases will have to be upgraded according to Ref. [2]. The PEM also has 960 phototubes, however those bases already have a dynode output designed into the base, so no modification is required. The CEM bases will be modified by the TAMU group. We estimate that the time required to modify the CEM bases is close to 1200 hours, *i.e.*, 30 man-weeks.

The electronics requirements are similar to those for the HADTDC system. The equipment needed is detailed in Ref. [1] and summarized in Table 1. It includes 48 Transition cards, 48 ASD cards, 24 TDC boards, a TDC crate, and around 2000 cables. It our understanding that there is slot space available on the detector and rack space in the counting room, along with a spare crate, tracer, and power supplies. No new technology needs to be researched or developed. Everything re-uses equipment or designs.

Table 1 gives the effective total cost in additional outlay from the collaboration/FNAL. The most expensive items are the ASD's and these will be covered by the Italian group from Frascati[1]. They thus represent no additional cost to FNAL or DOE. The second most expensive items in the table are the TDC's. These will be recycled using the "small-via TDC's" which are currently not going to be used. The current feeling is that they can be used in this project since they can be put upstairs where they can be easily accessed for repairs if necessary. Thus, these items have no effective cost to the collaboration, and in fact should be seen as a plus since these might otherwise be thrown away. The next dominant cost are the cables from the ASD's to the TDC's. We can get cheaper and more flexible cables which have a slower rise time than those in the HADTDC system. While they give us less resolution (and thus rejection power) they do not affect the efficency. We have also initiated conversations with other collaborations/experiments to see if we can reuse any of their cables (or other materials). In the interests of conservativeness, we have not included any cost savings from these sources. The next dominant cost are the crate and associated costs. Many of these can be taken from spares and effectively only have accounting costs. Finally, the transition boards were made at FNAL, and assembled at Michigan State University. It is our understanding that making another 50 of these boards is straight-forward. Great pains have been made to significantly reduce the effective cost to the FNAL; as discussed below, further possibilities exist.

The primary role of collecting the parts, testing, installing, commissioning, and maintaining the system would come from the TAMU group, and be supervised by D. Toback and T. Kamon. R.G. Wagner has committed to help train and supervise any part of the labor done at ANL, and H. Frisch has done the same at Chicago including any electronics design as needed. It is hoped that FNAL would help by contributing technical expertise.

[1] We are investigating whether ASD's are needed in fact at all.

Table 1: Cost estimate for instrumenting the CEM and PEM calorimeters with timing signals. The items marked with a * will be covered by one of the institutions. The items marked with a † will be recycled and have no effective cost to the collaboration, and in fact should be seen as a plus since these might otherwise be thrown away. The items marked with a ♣ can be taken from spares and effectively only have accounting costs. The effective costs listed below include all costs except the ASD's, TDC's and crate electronics which have no effective cost to FNAL. The Trigger Tower only solutions cut in half the number of cables from the ASD, patch panels, patch panel to TDC cables, and TDC's.

Item	Number reqd.	Unit cost	Total cost
CEM Bases			
Ground isolated Lemo connectors	960	6	6000
50Ω Lemo terminators	960	10	10000
Wire	960	nil	nil
Shrink tubing	960	nil	nil
Cables			
PEM PMT base to ASD	960	14	13000
CEM PMT base to ASD	960	14	13000
PEM ASD to TDC Patch Panel	144	200	28800
CEM ASD to TDC Patch Panel	144	200	28800
PEM TDC Patch Panel to TDC	48	209	10000
CEM TDC Patch Panel to TDC	48	209	10000
Electronics			
PEM 48 channel Transition Card	24	170	4080
CEM 48 channel Transition Card	24	170	4080
PEM 48 channel ASD boards	24	2800	67200*
CEM 48 channel ASD boards	24	2800	67200*
PEM 96 channel TDC boards	12	4800	57600†
CEM 96 channel TDC boards	12	4800	57600†
1st floor Crate, Tracer, Processor and Power Supply	1	15000	15000♣
PEM Patch Panels	12	500	6000
CEM Patch Panels	12	500	6000
Effective Cost (CEM + PEM)			139760
Effective Cost (CEM Only)			77880
Effective Cost (CEM Trigger Towers Only)			48980
Effective Cost (PEM Trigger Towers Only)			32980

4.5 Work Required Prior to Start of Run IIb

While the purchase of the electronics boards could be staged according to available funding, several items need to be completed before the beginning of Run IIb. This includes modification of the CEM bases to provide the dynode output, and termination and installation of all cables. It would also include the installation of the transition and ASD as well as the crates and patch panels for the TDC boards, as well as the boards themselves. We envision installing the upstairs hardware during Run IIa as it becomes available. We will try to install the cables during various shutdowns as time allows, and modify the phototube bases during shutdown between Run IIa and Run IIb.

4.6 Possible Options which Reduce the Project Cost

We feel that the physics motivations justify the cost of this proposal. However, if these costs are still considered too high, we can easily scale back the proposal to make it far cheaper, and still well worth doing, but with a far reduced acceptance. We summarize the possibilities here. The cost savings are itemized in Table 1.

1) We could use EM trigger towers instead of EM towers. This would cut in half the number of long cables from the ASD's to patch panels, and patch panels to TDC's.

2) We are investigating sending the signals directly from the phototubes to the TDC's, possibly with passive pulse-shaping. While the rise times would clearly not be as sharp (hurting our resolution) it would mostly likely only marginally affect our efficency.

3) We could instrument only the CEM. This would cut the cost nearly in half (only the CEM bases need to be modified).

4) We could instrument only the PEM. This would cut the cost nearly in half and no bases need to be modified. This clearly is less desirable as most of the interesting physics is expected to be in the central. However, it is true that we have at least some handles in the central and this extends that coverage. We could also begin here during Run IIa, and not affect the run.

4.7 Summary and Conclusions

To summarize, we propose augmenting the readout of the central and plug electromagnetic calorimeters for Run IIb to include timing information by adding hardware similar to that in the HADTDC system. This upgrade would significantly improve the potential of the CDF detector to do physics in samples with photons in the final state in two main ways: 1) It would reduce the cosmic ray backgrounds for important and difficult searches and measurements in a way which allows for significantly lower E_T thresholds, larger η acceptance and with a flat efficiency as a function of E_T; 2) It gives a vitally important handle that helps confirm that all the photons in unusual events, such as the $ee\gamma\gamma\not{E}_T$ candidate event, are from the primary interaction. With sufficient calibration data, there is even the possibility of searching for very long-lived particles which decay into photons.

We believe there many significant physics justifications for this project. There is no new technology which needs to be developed so there are no technical risks. The primary obstacle to this project before Run II was a man-power issue; this has been addressed. There has been an agreement from TAMU to provide technical work and supervision. There is an agreement from Frascati to provide ASD cards. It is foreseen that TDC's can be procured. The only remaining costs are cables and parts of the CEM bases. It is hoped that since these are small cost, finances (or spare parts) can be found for them as well. Ultimately, the bottom line is that for a modest cost and no technology risk, we can significantly extend the discovery potential for certain types of new physics.

References

[1] D. Toback *et al.*, "Proposal to Add Timing Information Into the Readout of the Central and Plug Electromagnetic Calorimeters," CDF Note 5518.

[2] H. Frisch, C. Grosso-Pilcher, and R. Wagner, CDF Note 4694; H. Frisch and R. Wagner, "CEM Phototube Base Modification for a TDC Dynode Output," CDF Note 4631; Peter Onyisi, "Efficiency of central and wall hadron timing information for cosmic ray discrimination for Run 1," CDF Note 5460.

[3] CDF Collaboration, F. Abe *et al.*, Phys. Rev. Lett. **81**, 1791 (1998) and Phys. Rev. D **59**, 092002 (1999); D. Toback, Ph.D. dissertation, Univ. of Chicago (1997).

[4] "Limits on Extra Dimensions and New Particle Production in the $\gamma \not\!\!E_T + X$ signature at CDF"; "Search for New Physics in Events with a Photon and b-quark jet at CDF"; "A Search for New Physics in Photon-Lepton Events in $p\bar{p}$ Collisions at $\sqrt{s} = 1.8$ TeV"; "Search for Narrow Diphoton Resonances and for $\gamma\gamma + W/Z$ Signatures in $p\bar{p}$ Collisions at $\sqrt{s} = 1.8$ TeV."

[5] D Collaboration, S. Abachi *et al.*, Phys. Rev. Lett. **78**, 3640 (1997).

[6] J. L. Rosner, Phys. Rev. D **55**, 3143 (1997).

[7] U. Baur, M. Spira, and P. M. Zerwas, Phys. Rev. D **42**, 815 (1990).

[8] A. D. De Rujula, M. B. Gavela, P. Hernandez, and E. Masso, Nucl. Phys. B **384**, 3 (1992).

[9] M. Baillargeon *et al.*, "Anomalous couplings and chiral lagrangians: an update," Proceedings of the Physics with e^+e^- Linear Colliders Workshop, hep-ph/9603220 (1996).

[10] N. Arkani-Hamed, S. Dimopoulos, and G. Dvali, Phys. Lett. B **429**, 263 (1998).

[11] A. Brignole, F. Feruglio, M. L. Mangano, and F. Zwirner, Nucl. Phys. B **526**, 136 (1998); Erratum-ibid.B **582** 759 (2000).

[12] H. Haber, G. Kane, and T. Sterling, Nucl. Phys. B **161**, 493 (1979); A. Stange, W. Marciano, and S. Willenbrock, Phys. Rev. D **49**, 1354 (1994); M.G. Diaz and T. Weiler, preprint VAND-TH-94-1 and hep-ph/9401259 (1994); A.G. Akeroyd, Phys. Lett. B **68**, 89 (1996).

[13] S. Ambrosanio *et al.*, Phys. Rev. Lett. **76**, 3498 (1996).

[14] S. Dimopoulos, M. Dine, S. Raby, and S. Thomas, Phys. Rev. Lett. **76**, 3494 (1996).

[15] J. L. Lopez and D. V. Nanopoulos, Mod. Phys. Lett. A **10**, 2473 (1996).

[16] For example, see S. Ambrosanio, G.L. Kane, G.D. Kribs, S. Martin, and S. Mrenna, Phys. Rev. **D** 54, 5395 (1996).

[17] D Collaboration, B. Abbott *et al.*, Phys. Rev. D **62**, 092004 (2000); D Collaboration, B. Abbott *et al.*, hep-ex/0011067 (submitted to Phys. Rev. D); D Collaboration, B. Abbott *et al.*, hep-ex/0011071 (submitted to Phys. Rev. Lett).

[18] S. Kuhlmann, "Timing Information For Central Photons and the ee$\gamma\gamma$MET Event," CDF Note 4256 (1997).

5 CSX Replacement

5.1 Introduction

The CDF collaboration proposes the eventual replacement of the existing CSX scintillators. These scintillators are part of the muon detection system in the pseudorapidity interval between 0.6 and 1.0. This proposal addresses a concern that the scintillator transparency may degrade during Run IIa to the point where the efficiency of the counters will be adversely affected. These counters were installed to provide a means of correlating a beam crossing with a hit in the muon chambers, so that false, out–of–time triggers at Level 1 could be avoided, and not contribute to the Level 1 trigger rate. This capability could be important if the accidental rate of out–of–time hits is too high. It should be noted that an additional use of the CSX counters was found in Run I to reduce the trigger rate due to interactions in the beam pipe and forward calorimeters. The necessity and effectiveness of the system for this purpose is not yet fully known for Run II, since the geometry is now quite different.

This project is being pursued by J. Budagov, M. Iori, D. Kim, T. Lecompte, G. Pauletta, M. Schmitt and G. Velev from Dubna, Bologna, KCHEP, Argonne, Trieste/Udine, Northwestern and FNAL respectively.

5.2 Concerns About Aging

The CMX (Central Muon Extension) arches span 270 degrees in azimuth and cover the region $0.6 < \eta < 1.0$. They comprise 8 layers of drift chambers, sandwiched between 2 layers of scintillation counters (CSX, Central Extension Scintillators) which are read out from opposite ends for accurate timing. Good timing resolution ~3 ns was critically important for background rejection in Run I. In Run II it will also serve to identify bunch crossings because the chamber drift time (1.4μs) is longer than the 132 nsec interval between collisions. The 1.8 m - long counters were constructed from 2 cm - thick NE114 (now BC 416) scintillator [1], as were the longer (3.2m) CSP (Central Upgrade Scintillator) counters which cover the vertical walls of the central region.

Evidence of inefficiency (~83%) in the CSX turned up in the course of Run I [2]. Similar measurments showed that the CSP were also inefficient(~92%). These measurements prompted an investigation which eventually revealed that the counters were aging prematurely, a condition which was manifest when the counters were unwrapped: the scintillator was found to be yellow, a condition which usually corresponds to a loss of transparency at the scintillator emission wavelength and that can also correspond to a loss of brightness. Measurements of the transmittance of scintillator samples showed a bulk (not surface) loss of transparency at the scintillator emission wavelength (between 410 nm and 480 nm for NE 114).

These effects can be brought about by radiation damage but estimates of the accumulated dose (based on TLD measurments) exclude radiation as the principal cause of aging. This conclusion is supported by the observation that a number of spare CSXs, which had been kept in the warehouse and had therefore never been exposed to the beam, are subject to the same effects. It is therefore reasonable to conclude that that premature aging had occurred and that, since it is a bulk effect, it probably corresponds to oxidation of the color centers due to poor deoxigenation of the scintillator during the manufacturing process.

In order to evaluate the effect of this deterioration in quantitative terms it was necessary to measure the light output in absolute terms and to evaluate the rate of deterioration so as to understand the counters' present and future limitations. We focussed our attention on the longer CSPs which, because of their length, were better suited to measurements of attenuation length. The results of these studies are summarized in the next section. Because they refer to the same scintillator, they are relevant to both CSP and CSX.

5.3 Scintillator Aging Studies and Projections

After calibrating our DAQ system by single photon counting [4], the absolute light output, *i.e.* the number of photoelectrons reaching the PMT photocathode when a counter is traversed (normally) by a cosmic muon, was measured as a function of distance from the PMT. The results of such measurements for three counters are shown in Fig. 15. The full circles represent the data taken with one of our deteriorated CSP counters ("30 NW" for counter No. 30 on the West end of the North Wall). The open circles are the data from an identical CSP counter ("Test counter 32"), made of *undeteriorated* NE114. The third data set was taken with a CSP counter made of new polystyrene-based scintillator [5].

The deterioration of "30NW" is evident. Other counters were also measured and the results for a representative number of them are similar, with fluctuations of $\sim \pm 30$ % , corresponding to: (1) fluctuations in the photoefficiency of PMTs and(2) in the scintillator quality (purchasing records indicate a fluctuationsof ± 30 % from batch to batch).

In order to evaluate the rate of deterioration and to distinguish between deterioration in brightness and in attenuation, we compared the output of the aging counters to that of the undeteriorated NE 114 (test counter 32) at two points: the "near end" (*i.e.* that closest to the PMT), evaluated by extrapolating the data backwards as shown in Fig. 15 and a point 20 cm from the far end (*i.e.* 300 cm from the photocathode). For the period 1992 - 1998 (Δt = 6 years) we define

$$\begin{aligned} N_{x,0} &= \textit{light output at } t = 0 \\ N_{x,6} &= \textit{light output at } t = t + \Delta t \end{aligned}$$

where $x =$ "near" or "far". Then, assuming the deterioration is exponential, *i.e.*

$$N_{x,t} = N_{x,0} \exp - \Delta t / \tau_x$$

we use the data N_{x0} and $N_{x,6}$ to calculate a "deterioration lifetime" τ_x for both ends

$$\tau_x = \Delta t / \ln \left(N_{x,0} / N_{x,6} \right)$$

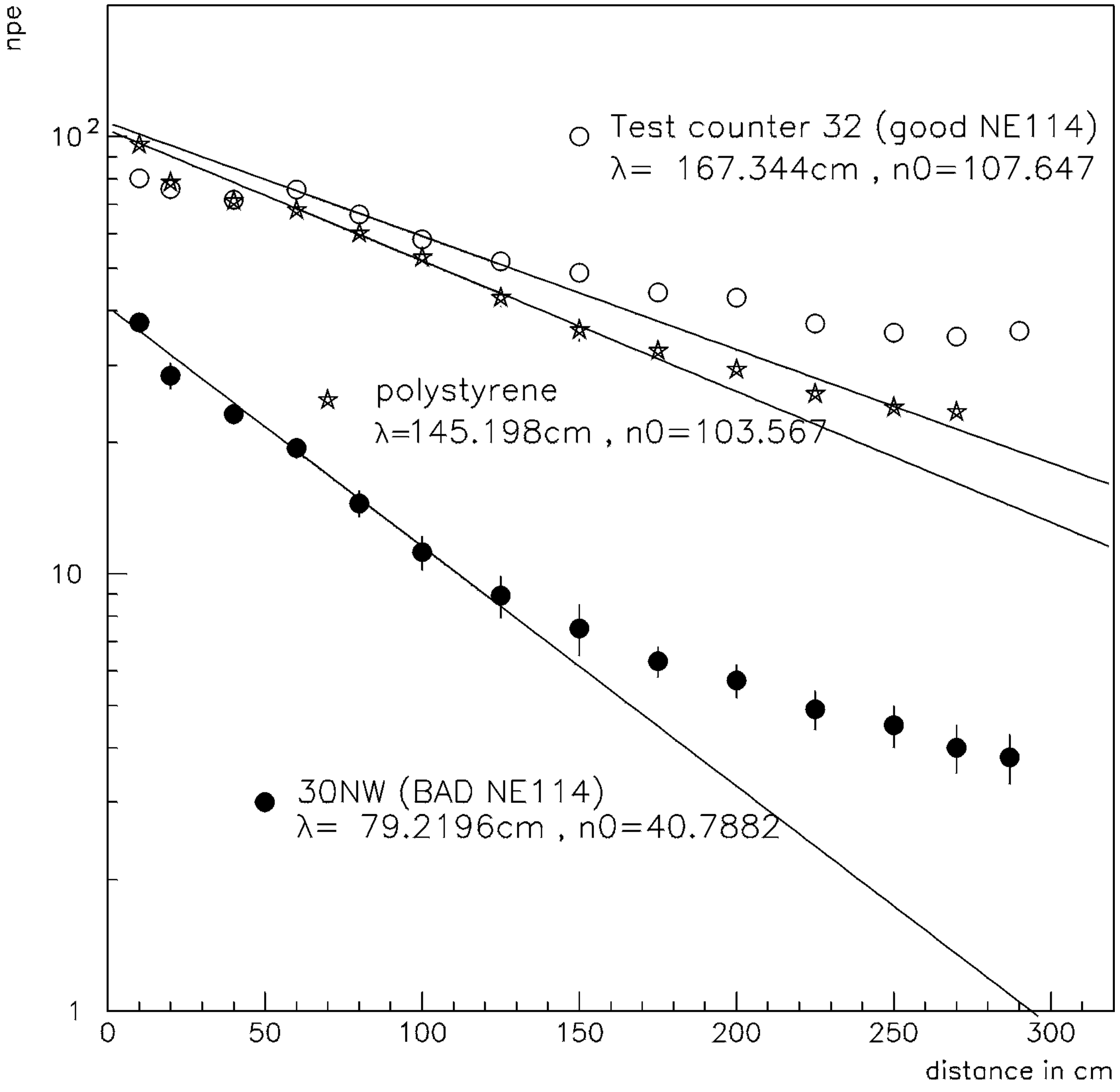

Figure 15: Absolute light output (i, p.e. per muon) as a function of distance from the PMT (in cm), for three different CSP counters: "Test counter 32", made from NE114 (good), "Russian Prototype" made from polystyrene-based scintillator (good), and "30NW" (aged).

If, for the near end, we use $N_{near,0} = 105$ $p.e.$ and $N_{near,6} = 35$ $p.e.$, and for the far end we use $Nfar, 0 = 40$ $p.e.$ and $N_{far,6} = 5.5$ $p.e.$, we obtain:

$$\tau_{near} = 6.2\ years,\ i.e.\ 15\%\ per\ year$$

$$\tau_{far} = 2.9\ years,\ i.e.\ 30\%\ per\ year$$

Using these "deterioration" constants, we then estimated that, by the end of 2003 , the counter output at the far end would be reduced to 0.7 $p.e.$ Assuming poisson statistics and a discriminator threshold of 1 $p.e.$, this would correspond to less than 50 % efficiency.

On the basis of this information, it was decided to intervene and a scheme was devised for refurbishing the "wall" CSP counters by adding wavelength - shifting - fiber to one side. For more information on this procedure, the reader is referred to [7]

Our evaluation of the deterioration rate is obviously subject to several sources of uncertainy. Fluctuations in the scintillator quality and PMT efficiency are statistical and mean that some counters are not going to deteriorate as fast, but that others will do so faster. This in fact represents a *more dismal* situation because some counters will start dropping out before the time projected on the basis of the averages reported above. The "systematic" uncertainties derive from the uncerainty in the actual period of deterioration (e.g. the date of production is uncertain by almost a year) and our assumptions regarding its initial performance (see above). We estimate that these uncertainties could influence our estimates of the deteroration rate by about $\pm$ 30 %.

Because the CSX are shorter (1.8 m vs. 3.2 m) they do not suffer as badly from deterioration in counter transparency. On the basis of the above measurments, we would expect ~ 8 $p.e.$ from a cosmic at 20 cm from the far end. However, because they are shorter, we can expect more light from the reflected component. In fact, from bench measurents on 19 counters, we obtained between 10 and 14 $p.e.$. This is sufficient to make the probability of zero negligible, *i.e.* for it to be possible to obtain full efficiency by increasing the PMT gain. We therefore embarked on the task of re-plateauing the counters one by one, in situ, using cosmic muons. At the same time we measured absolute output at the far end by substituting, wherever possible [9], the counter's PMT with one that had been calibrated using the method outlined in the above section. This work is summarized in [8]. Note that the averages are lower than measured on the bench. This is due to a systematic error in the cable attenuation and because the photoefficiency of the calibrated PMT was lower than the average photoefficiency. For a correct interpretation of these data, their averages should be renormalized to 12 $p.e.$.

Deterioration rates at the far end of the CSXs were evaluated from the data taken at the middle (*i.e.* 160 cm from the photocathode) of the CSPs. This obtains a deterioration rate of 25% *per year*. The light output from the far end of the CSX counters at the end of 2003 can be expected to be 12 $p.e.$ $(0.75)^5 = 2.9$ $p.e.$, i.e. $< 95\%$ and, since we need a coincidence of two counters, the efficiency drops to 90%. In 2004 it would be $< 77\%$ and in 2005 $< 58\%$.

It should be emphasized that, for all of the above estimates, we have taken the inefficiency to be the probability that one observes zero photoelectrons. This assumes that one would be able to operate with a threshold of one photoelectron. In fact, this mode of operation is very susceptible to noise and it may not be possile. More reliable estimates would be obtained by putting the limit of operability at 2 photoelectrons. In this case, inefficiencies will turn up a lot sooner.

Finally, we address the supposition that the construction of the new shielding "snouts" might make us less dependent on the CSX. The background affecting the CSX during Run I originated mainly from interactions of the beam with the plug and the toroids. The snout was introduced to reduce it. The commissioning run showed that we do indeed get singles suppression factors of ~ 3 between shielding in/shielding out situations. However, encouraging though this preliminary result might be, it does not imply that the background has been suppressed by a factor of 3 with respect to Run I because the geometry has changed. (e.g., the additional material due to the new plug's extended η coverage will produce additional background) and could well change further if the miniplug is installed. The truth is that we do not yet have a reliable estimate of the background.

We conclude this section by emphasizing that we cannot count on these counters surviving Run II and that the evidence we have outlined above does not support optimism.

5.4 Proposed Course of Action

It is clear that we cannot refrain from acting in the hope that aging *might* have stopped. We plan to optimize our means of monitoring the response of the CSX counters. A monitoring strategy would include sending the outputs of a sample of counters to ADCs and installing a number of test counters before and behind a sample of counters to enable quick and continuous monitoring of their efficiency. Most importantly, we must arrange to monitor efficiencies and backgrounds closely by looking at real data *e.g.* $J/\psi \rightarrow \mu\mu$.

In order to minimize the time to return to routine running conditions, the baseline plan will be for a scintillator for scintillator replacement of the CSX counters, with an estimated cost of $150K. The detailed plan requires further engineering studies and can preferably wait until we can do it on the basis of further evidence regarding the rate of deterioration and the importance of the CSX for background rejection and crossing identification. However, we want to be careful that the long lead times involved in planning and funding do not compromise our ability to implement the remedy should the worst come to worst.

References

[1] Bicron Corp.

[2] P, Giromini, A. Gordon, D. Kestenbaum, G. Michail, P. Schlabach and J. Troconiz, CDF Note **3898**.

[3] G. Velev, private comm.

[4] E.H. Bellamy et al., N.I.M **A339**,468 (1994)

[5] UPS 93 A, made by Monokristal, Ukraine.

[6] E.H. Bellamy et al., N.I.M **A343**,484 (1994).

[7] S. Cabrera et al., N.I.M **333**, 333, 2000.

[8] J. Fernandez et. al., CDF Note **5006**.

[9] This was not done for the external counters because the support structure makes it virtually impossible to access the counters. I. Crotty et al. Nucl. Instr. and Meth. A 337 1994 370

6 Adding Stereo Segment Finding and 3D XFT Tracking in the Trigger

6.1 Introduction

The trigger for Run II incorporates tracking in the Level 1 trigger decision. The tracks are found by the eXtremely Fast Tracker (XFT) and the resulting track list is sent to the extrapolation crate (XTRP) for distribution and matching with other Level 1 primitives. The XFT track list is also sent to the SVT for identification of displaced tracks at Level 2. The XFT identifies tracks in r-ϕ only, using the four axial layers of the COT. However, since both the electron and muon subsystems are segmented in z, the ability to extrapolate and match XFT tracks in the z view could prove extremely useful in reducing fakes. In addition, a single z measurement allows a coarse estimate of $\cot\theta$, which in turn allows a multi-track mass calculation at the trigger level.

The CDF collaboration proposes to add a single stereo measurement [1] to the existing XFT 2D tracks. The stereo measurement would be made in the outermost stereo layer (SL7), using the same segment Finder approach already implemented for the four axial layers. The approach would share many features with the existing XFT system:

- The TDC mezzanine cards are the same. The cards needed for hit finding in SL7 already exist.
- There are enough ansley cables available to bring the SL7 hit data to the first floor counting room.
- The TDC and Finder transition cards would be very similar to those in use for the current XFT system.
- The Finder boards themselves would also use a similar design, although the output section would be different. The algorithm to find stereo segments is identical to that used in the axial layers (and versions of the SL7 mask set already exist).

There are a number of ways in which the stereo segments can be attached to an existing XFT 2D track. We describe two primary options below: one which makes the resulting 3D tracks available in time for the Level 1 decision[2], and a second in which the 3D tracks are available at Level 2. In the sections below, we give an overview of the physics motivation, a description of stereo segment finding, and an outline of the two options for 3D track finding and their use in the trigger.

This project is being pursued by Richard Hughes, Phillip Koehn and Brian Winer of Ohio State University and Jonathan Lewis of Fermilab.

6.2 Physics Justification

There are two motivations for finding stereo segments in the XFT:

- Stereo segments used in the Level 2 processor can help reduce lepton fake rates by showing that tracks are associated with muon chambers and/or calorimeter towers. In addition, stereo segments can be used to reduce the dimuon trigger rate if a mass for J/ψ candidates can be calculated in the Level 2 processors.
- Stereo segments attached to XFT tracks early in the electronics chain can be used to calculate masses in an upgraded two-track trigger system for Level 1.

6.2.1 Impact on Level 2

The addition of stereo information can reduce Level 2 trigger rates for many trigger signatures. We consider two examples: CMX muons and $J/\psi \to \mu^+\mu^-$. For CMX muons, we require at Level 2 the association of a SL7 segment with an XFT track that is consistent with pointing to the CMX. Further, we can require the SL7 segment to pass a high-p_T threshold. The same approach can be used for η-gap muon triggers and for electron triggers, where a SL7 segment must be consistent with a track projecting to the seed tower of an electromagnetic cluster. Similar pointing cuts might also be used for tau triggers. In all cases, the 30 cm r.m.s. spread of the z position of the primary interaction vertex sets a limit on the required precision on the z measurement. For $J/\psi \to \mu^+\mu^-$ triggers, we consider CMU-CMU pairs and use all the SL7 segments that can be associated with each XFT track to form mass hypotheses. Candidates consistent with the J/ψ mass would be accepted. Since the tracks are typically low-p_T, SL7 segment slope pointing may also improve the rejection. Good mass resolution can be achieved because the uncertainty in the primary-vertex z position does not translate into a large uncertainty in the opening angle between the two muons.

Using test data from Run I, we have estimated the cross section for CMU-CMU dimuon triggers with and without a mass cut. For this study we used the hit-level CTC-XFT simulation. In order to extrapolate to the Run 2 muon threshold of 1.5 GeV/c, we have fit a power law to the inclusive dimuon trigger and SL7-mass trigger cross sections as a function of muon-track threshold. The stub timing cut is fixed at 200 ns. The result is shown in Figure 16. Although the extrapolation error is surely large, one draws the clear impression that the cross section for an inclusive dimuon trigger with a threshold 1.5 GeV/c may be enormous, without requiring a mass window cut. The extrapolated cross sections are 160 nb for the opposite-charge trigger and 20 nb for the mass trigger. Based on Run 1 experience, we can estimate that a fully inclusive dimuon trigger without the charge cut and including CMX would probably have about a factor 4 higher cross section (640 nb) which corresponds to 125 Hz at 2×10^{32} cm^{-2}s^{-1}. The mass trigger rate including CMX is probably a factor of 2 higher than the CMU-CMU trigger estimates here, or 8 Hz at 2×10^{32} cm^{-2}s^{-1}. Thus, the cross section for a trigger with a mass cut should be well-controlled, and it will be possible to have a highly efficient $J/\psi \to \mu^+\mu^-$ trigger at the lowest possible momenta.

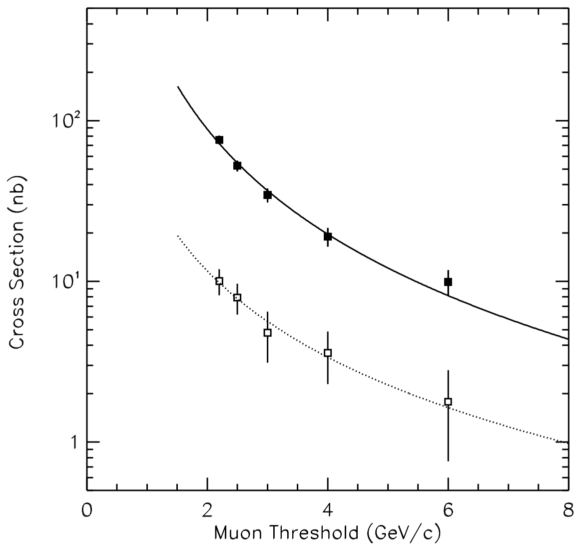

Figure 16: Dimuon trigger cross section vs. instantaneous muon threshold. Solid points are for tightly matched opposite charge pairs. The open squares are the SL7 mass trigger rates. The fit is to a power-law form. The points are not strictly independent, but the trend is clear.

We have estimated the improvement in trigger rates for inclusive 12 GeV/c CMX muons using again test data from Run I. We consider only those events that a trigger with a bin 2 (nominally 3.4 GeV/c) CFT track matched to a high-p_T CMX trigger stub. The cross section estimates have been scaled for the increased CMX coverage in Run 2. Figure 17 shows the results of the study. Requiring a SL7 segment consistent with a track projecting to the CMX lowers the trigger rate by about a factor of 2. Requiring that it be a high-p_T segment gives another factor of 2. However, some of the reduction may be due to the fact that the SL7 segment comes from a good offline track its existence may in and of itself reduce the fake rate. Also, improved shielding of the CMX from the beam line should lower trigger rates as well, so the additional factor from the track z matching may not be as large as is estimated here.

The two studies described above highlight the capabilities of stereo segments. The prediction for the CMX at 12 GeV/c corresponds to a rate of 20 Hz at a luminosity of $2 \times 10^{32}\,\mathrm{cm}^{-2}\mathrm{s}^{-1}$ which would ensure that the CMX trigger could be fully efficient and would not require a prescale at the highest luminosities. The factor of 8 reduction in opposite charge dimuons with the J/ψ mass cut is highly efficient ($> 93\%$). The SL7 mass trigger should be well-behaved at the lowest possible muon threshold and the highest luminosities, ensuring full efficiency for $J/\psi \to \mu^+\mu^-$ decays.

6.2.2 Impact on Level 1

A new possibility which depends on the 3D XFT is the CDF Track Trigger 2 [2], which would allow a mass trigger in Level 1. One of the main purposes of the two-track trigger is to

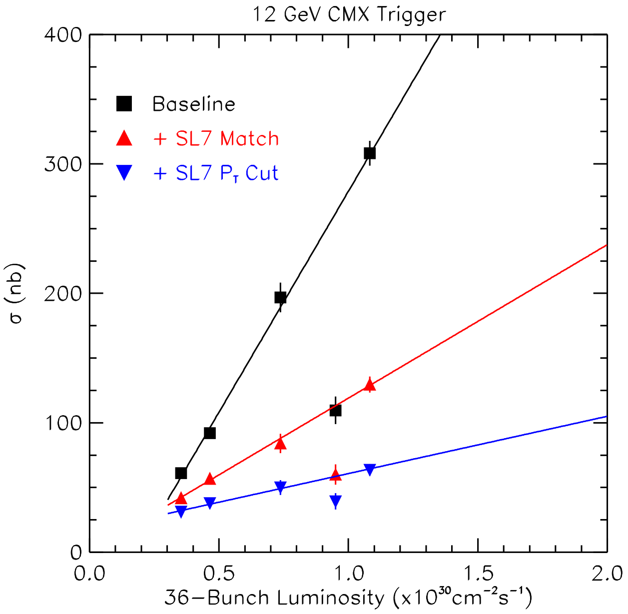

Figure 17: Estimated trigger cross section for 12 GeV/c CMX muons. Upper line and points do not include SL7 z information. The lower sets include all segments or only high-p_T segments. The points just below 1×10^{32} are excluded from fit because of a probable luminosity counting problem.

collect events with the decay of B mesons into just two final-state stable mesons: $B^0 \to \pi^+\pi^-$, $B^0 \to K^\pm\pi^\mp$, $B_s^0 \to K^\pm\pi^\mp$, and $B_s^0 \to K^+K^-$. Trigger rates and event yields were studied in CDF 4095 [3]. To accommodate the higher instantaneous luminosity of Run IIb, the nominal two-track trigger cuts would need to be tightened substantially, reducing the signal cross section by a factor of two. However, a recent study [4] has shown that in 2 fb^{-1}, using the $B \to h^+h^-$ modes, CDF can measure the CKM phase γ to $10°$. While interesting, this level of precision does not provide a stringent test of unitarity of the CKM matrix. Further study in Run IIb would be desirable if the event yield can be substantially increased. The cuts on the XTRP's two-track trigger result in many events beyond the mass range that is needed to study the $B \to h^+h^-$ modes. These events do contain many interesting B events, but we want to optimize for the relatively rare dihadron mode. Because the backgrounds in the 4-6 GeV range are quite low, a mass trigger would be ideal. Furthermore, if an improved two-track trigger were capable of using tracks down to the XFT's threshold of 1.5 GeV, the efficiency for $B \to h^+h^-$ decays would be greatly enhanced even beyond the Run IIa trigger. The exact improvement must be the subject of further study. The addition of a two-track mass trigger would then be used exclusively for the h^+h^- decays and the original 2D two-track trigger might continue to be used for more inclusive B studies. While the lowering of the p_T threshold for the B daughters clearly increases the efficiency of the Level 1 trigger, it is only useful if the capability of Level 2 is also improved. Although further study is required, improved knowledge of the performance of the SVT indicates that it will likely be possible to lower the SVT threshold to 1.5 GeV without substantial loss of efficiency[L. Ristori, private communication]. Thus stereo tracking in Level 1 holds the key to a possibly four-fold increase in the $B \to h^+h^-$ efficiency over what might otherwise have been achieved, and an order of magnitude improvement in yield over Run IIa.

6.3 XFT Stereo Segment Finding

Below we summarize the design and implementation of segment finding in the stereo layers of the COT. This design is very similar to the axial layer segment finding of the existing XFT system. Documentation of the XFT can be found on the web [5] and a more detailed description of stereo segment finding is in CDF 4300.

6.3.1 Design

In the current XFT system, the Finder searches for high-p_T track segments in each of the four axial superlayers of the Central Tracker. Each found segment is characterized by a mean ϕ position in the axial superlayer, called a pixel. Pixels are found by looking at TDC hit information in four neighboring COT cells and making a comparison to predefined sets of hit patterns, or "masks", that are consistent with good track segments. A mask will change depending on the ϕ of the track and its angle through the cell (or p_T). All possible masks for tracks with $p_T \geq 1.5$ GeV/c are part of the Finder PLD design for a given superlayer. Every 132 nsec the Finder outputs 12 bits per cell (12 pixels for the inner two axial layers, 6 pixels times 2 slopes for the outer two axial layers) to the Linker system.

The stereo segment finding works almost exactly like the segment finding for the axial layers. In defining the masks, we assume that the stereo angle is zero. The total number of masks needed to identify track segments with p_T greater than 1.5 GeV/c is 300. As with the outer 2 axial layers (SL6 and SL8), we divide each cell into 6 pixels.

The measurement of the z coordinate of a track in a stereo layer of the COT requires an identified track in the r-ϕ plane associated with a measurement of the ϕ position of the track segment in the stereo layer. This association is performed by matching a pixel in SL6 of the track to a range of pixels in SL7. The range depends on the p_T (or curvature) of the track and the stereo angle. If the track passes through the stereo layer at a z coordinate other than z=0, there will be an apparent difference in ϕ between the extrapolated position of the r-ϕ track at the stereo layer (denoted ϕ_{exp}), and the measured ϕ position of the track segment in the stereo layer(denoted ϕ_{fnd}). The z coordinate is given by the following expression:

$$z = \tan\left(\phi_{exp} - \phi_{fnd}\right) \cdot \frac{1}{S} \quad (1)$$

where S is a constant dependent on the "stereo angle". For COT stereo layer 7, $S = 2.75 \times 10^{-4}$. Based on the expected resolution in ϕ_{exp} and ϕ_{fnd}, we can expect a resolution on z at SL7 of better than 6 cm.

6.3.2 Implementation

The Finders are implemented using Altera's FLEX 10K-series programmable logic devices populating 9U VME cards. By definition, a single Finder PLD looks for valid track segments in each of 4 neighboring COT cells. Since the total number of cells in SL7 is 432, the required number of Finder PLDs is 108. Due to the size and inflexibility of the Ansley cables, we are limited to a practical maximum of 8 Finders per board. We plan to use 6 Finders per board. This makes each board identical, and also allows room for the circuitry needed to format the data before sending it to other Level 1 or Level 2 boards (described in section below). Using 6 Finders per board, we need a total of 18 stereo Finder boards. Since each VME crate has 21 slots, of which 2 are taken up by the controller and tracer, we can fit all the stereo Finder boards into a single crate.

Many parts the existing XFT Finder system design may be used for stereo segment finding without requiring any changes. These include the TDC mezzanine card, TDC transition module, Ansley cables(we have enough in hand), Finder transition module, and the Finder cPLDs. However there are some changes. A new Finder backplane will be needed as it is responsible for routing neighbor wires from slot to slot. The data input section and Finder cPLD section of the Finder board will remain the same, but the output data driving sections will need to be changed. On the axial Finder boards, National channel links are used to drive the output to the Linker boards. This should be replaced with a design to drive the data to Level 1 or Level 2 boards.

Table 2 details the cost for the production Stereo Segment Finding system. Most of the cost is in the purchase of boards already designed for the XFT2D system. The number of spares includes those needed for test stands. The cost for any additional hardware for implementing a mass trigger in Level 1 or Level 2 is not included.

6.4 Option 1: Linking Stereo Segments in Level 1

Currently the crate in 1RR27F-B has been allocated to XFT stereo tests. We presume this would be the stereo XFT crate if the ultimate proposal were approved. To include stereo information in Level 1, we would replace the Linker Output Modules (LOM), which simply buffer the linker output prior to shipping to the XTRP, with a new Stereo Association Module (SAM). Each SAM would take as input the track data from a linker and several cables of stereo segment data from the stereo finders using channel links. For the configuration we proposed in CDF4300, there would be 18 stereo finders, each one handling 20° of azimuth. Each one would have four channel-link based outputs, two copies for each 10° half of the board. Having the duplicates allows for overlaps in the regions in going from the 18 stereo finders to the 24 SAMs. The SAM would perform several functions

- Buffer output to send to XTRP in same format as LOM
- Associate the appropriate 36 bits of stereo data with each 2D XFT track, using look-up maps

Description	Production Quantity	Spares	Production Unit Cost	Production Cost
Finder Card Unloaded	18	6	$1,000	$24,000
Finder Discrete Components	18	6	$300	$7,200
Finder Altera chips	108	36	$145	$20,880
Input section chips	108	36	$100	$14,400
Output section chips	54	18	$100	$7,200
Finder Backplane	1	2	$1,800	$5,400
Finder Transition module	18	6	$600	$14,400
TDC Transition module	54	10	$600	$38,400
TDC Mezzanine Card	54	10	$600	in hand
Connector/Cables				$10,000
Stereo Association Module (SAM)			$4,000	$96,000
Total				$239,880

Table 2: Production cost estimate for the XFT3D system, segment Finding only.

- Pipeline and buffer the 3D tracks for readout by L2 and DAQ
- Provide tracks to the 3D two-track trigger system

To keep data transfers as short as possible, we imagine that the new two-track trigger would reside in the location directly above the stereo finder crate since it is as yet unallocated. By making the associations in the SAMs, the problem is made parallel, so the work can be done in a time consistent with the requirements of the Level 1 decision. In addition to the SAMs and the 3D-two-track trigger, we would need a new Track Master (TM) module to collect the track information from the SAMs and sparsify prior to sending to Level 2. The existing Level 2 track interface board can buffer the additional data. Although the design work for both the SAM and TM is not trivial, the new functionality of the SAM is very similar to the XTRP data board in that it is a track-based look up. The difference is that the data looked up is dynamic. The TM is quite similar to functions of the XTRP's clock control board, so again we can learn from the experience of the XTRP. At present it is difficult to estimate the cost of the SAM modules, but based on their functionality and using our experience with the Finder and Linker modules as a baseline, an estimate of $4,000 per board is not unreasonable.

6.5 Option 2: Linking Stereo Segments in Level 2

The original proposal for the use of stereo information had the stereo segments linked with r-ϕ tracks in the L2 processor. If we choose not to pursue the use of stereo information in the Level 1 track trigger, this option would still be available to us. This option is discussed in detail in CDF 4300; however, we summarize a few of the features here. First, the stereo pixels would need to transfered to an interface board residing in the L2 decision crate. The connection between the stereo Finder boards and the interface board would need to be optical links, to accommodate the amount of data and the distance that the signals must travel. This adds approximately an extra \$100 per driver/receiver pair compared with driving the information using standard LVDS circuitry.

The interface board would consist of memory to store the stereo pixel information until it was requested by the L2 processor. This board could be designed to be a general purpose L2 interface board which could be used for other purposes in the future. Once the data was received, it must be transmitted to the L2 processor via the 128-bit "Magic Bus". To transmit this data we could either transfer 2592 bits ($\sim$ 800 ns) or have the L2 processor poll the interface card for the specific bits (36) required for a given track. Which transfer protocol is used can be programmed into the L2 software and could depend on the size of the event. We have estimated the R&D costs for the interface board would be \$15,000 and the production cost at \$5,000 per board.

6.5.1 3D tracking performance

We have implemented a version of the stereo segment finding algorithm in the XFT standalone simulation. For both the axial layers and the stereo layer, the Finder is implemented using a database of masks. The association of SL7 segments to XFT2D tracks is done by considering all segments in a valid window around the XFT2D track. Details of this study can be found elsewhere [1], but as an example of the performance we consider the difference between the true z position and the XFT determined z position. This is shown in Figure 18 for a sample of simulated tracks. In this simulation, the track p_T was flat from 1.0 to 10.0 GeV/c. Tracks from an average of 2 minimum bias events were overlaid on these Monte Carlo events to simulate the effect of occupancy in the COT in Run II. These distributions do not degrade appreciably if the average number of overlaid minimum bias events is increased to 10. The z coordinate is given by equation 1. The uncertainty on the z position is determined by how well we measure the two phi positions. In this case, the uncertainty is dominated by the extrapolation uncertainty on ϕ_{exp}, which comes from the XFT2D track measurement errors on p_T and ϕ_{SL6}. The z position resolution is $\sim$ 6cm for the overlap of both the 2 and 10 minimum bias events.

6.6 Time Estimates

Much of the design and construction of the stereo upgrade to the XFT is based on experience of the current XFT system. The time requirements can be divided into several categories.

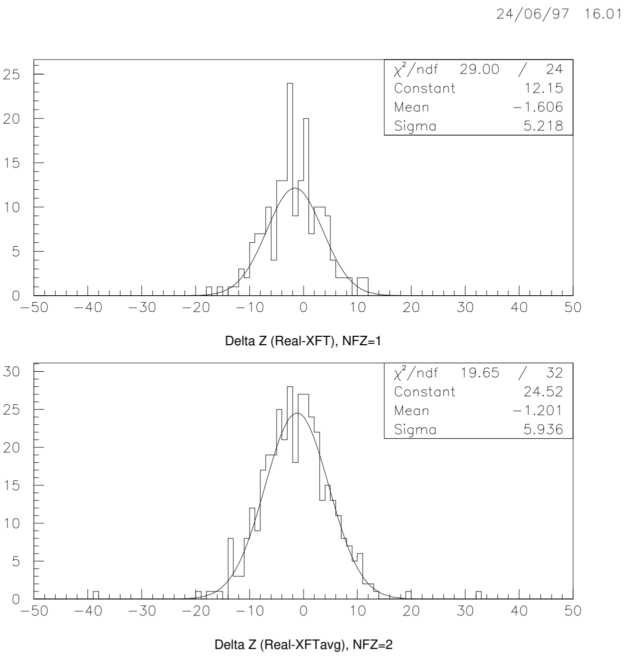

Figure 18: Top plot: Difference between the true z position and the XFT z position at outer stereo layer for one and only one valid stereo segment near XFT track. Bottom plot: Same when two valid stereo segments near XFT track. For both plots the average number of overlaid min-bias events is 2.

- **Board Design:**

  The COT transition cards and the hit finder cards for the TDCs already exist. The Stereo Segment Finder boards are based on the Axial Segment Finder boards with only minor modification to the output section of the board. These boards could be designed and assembled in $\approx$12 months. The Stereo Association Modules are a new design and would require more R&D. However, the task of these boards is not complicated and therefore we estimate $\approx$18 months for design and assembly. This could be done concurrently with the development of the Stereo Segment Finders.

- **Installation:**

  Installation will include *(i)* COT transition cards that must be installed in VME crates that reside on the detector, *(ii)* cables from the COT transition cards to the racks in the first floor counting room, and *(iii)* Stereo Segment Finders and Stereo Association Modules in the counting room. The first two items can be performed in parallel and would require down time of approximately 1-2 weeks. Installation of the VME modules in the counting room will require a negligible amount of time and will be performed incrementally as boards become available.

- **Commissioning:**

  Due to the modular nature of the system, part of the system can be installed and tested prior to the full completion of the parts. This will allow us to begin integration and commission of the system as soon as the first boards have been assembled. This approach worked very well with the XFT and allowed the first stages of commissioning to be completed prior to the full compliment of VME boards being finished. We estimate 4-6 weeks worth of commissioning with the first part potentially overlapping with the tasks listed above.

6.7 Conclusion

The extension of XFT from 2D to 3D, while not trivial, is a straightforward extension of ideas which we have put in place for Run IIa. Almost all of the hardware that would be necessary to implement the stereo Segment Finding portion of XFT3D have been tested with the present XFT Finder system. Adding stereo tracking in either Level 1 or Level 2 would allow both additional fake rejection (which could be significant in the higher luminosity environment of Run IIb) as well as the ability to calculate masses relevant for many B-physics studies.

References

[1] Hughes, Winer, Koehn, Lewis, Saltzberg, CDF4300, "XFT3D: A Proposal for Adding Stereo Segment Finding and 3D XFT tracking in the Trigger".

[2] N. Eddy, K. Pitts, M. Kasten, "Expression of Interest: CDF Track Trigger 2".

[3] Intae Yu and Jonathan Lewis; CDF4095 "Study of $B \rightarrow \pi^+\pi^-$ trigger rate for Run II".

[4] Frank Wuerthwein; CDF5271 "Measuring Gamma to better than 10degrees in Run II".

[5] http://cdfpc2.mps.ohio-state.edu/xft/xft_home.html

7 Track Trigger Upgrade

7.1 Introduction

One new aspect of the CDF-II Level 1 trigger system is the Track Trigger module. The Track Trigger module is the component of the Level 1 trigger that generates decisions based exclusively upon COT tracking information. The primary motivation for this trigger path is to select hadronic decays of B hadrons, with silicon impact parameter information (SVT) available at Level 2.

The challenge for the Track Trigger is one of rate: estimates are in the 20-40 kHz range. Rate reduction is of course possible, but at the expense of efficiency for the signal. The rate also grows with track multiplicity, therefore the Level 1 Track Trigger rate will continue to grow as the Tevatron luminosity increases.

In this document, we outline two possible upgrade paths to the Track Trigger. The motivation for considering upgrades to this system is twofold:

1. Allow for continued efficient operation at higher Run IIb luminosities
2. Improve the physics reach (better statistics, higher purity, more decay modes) of the all-hadronic B decay trigger.

Below, we summarize the functionality of the CDF Track Trigger that will be operational at the beginning of Run IIa. Following that, we propose two distinct upgrades to the Track Trigger that we believe are realistic and can improve the physics potential for CDF.

This project is being pursued by Nathan Eddy, Michael Kasten and Kevin Pitts of the University of Illinois.

7.2 CDF Track Trigger

The Level 1 Track Trigger is an adjunct to the XTRP system. It resides in the same VME crate as the XTRP and provides Level 1 triggers based on XFT track information only. The XTRP modules select tracks above a given P_T threshold (nominal 2.0 GeV/c) and passes them on a bus to the Track Trigger. The total number of tracks is counted. If more than 6 tracks are found an automatic Level 1 accept is generated. If there are 2-6 tracks, the P_T and ϕ information is used to interrogate look-up tables to generate various Level 1 triggers.

The Track Trigger operates synchronously with the remainder of the Level 1 trigger system and generates a decision on every beam crossing, regardless of occupancy and/or rate. Several triggers have been proposed and studies performed to estimate Level 1 trigger rates [1, 2, 3, 4]. Based upon these studies and the type of low-p_T physics the Track Trigger is attempting to accept, we know that the Level 1 rate from this trigger will be quite high, in the range of 20-40 kHz.

After sending out the Level 1 trigger information all tracks are put into a pipeline and stored pending the Level-1 trigger decision. If a Level 1 accept is received, the tracks are latched into Level 2 buffers. The tracks are then extracted and put into two separate FIFO's for delivery to the Level 2 processor and to the SVT respectively.

The Track Trigger decision is generated based upon the kinematic information from the tracks: transverse momentum (p_T), charge, azimuthal angle (ϕ) and isolation. The system will support up to 16 different types of triggers, but is limited to quantities calculated based upon pairs of tracks. Regardless of these quantities, the Track Trigger will generate an auto-accept if the charged track multiplicity is greater than six.

Functionally, the Track Trigger module uses lookup tables loaded into static RAM. These tables take advantage of the azimuthal symmetry of the tracking chamber and XFT. In order to perform these operations quickly, lookups for track-pairs are done in parallel. The Track Trigger looks at up to 15 possible pairs of tracks (all possible pair-combinations of up to 6 tracks) and generate up to 16 different trigger decisions.[2]

In addition to providing a Level 1 trigger path for all-hadronic triggers, the Track Trigger can provide back-up and control sample paths for lepton triggers.

7.2.1 Status

The Track Trigger board has completed initial test and debugging in the XTRP test stand in Urbana. The Track Trigger has been moved to B0 and integration tests have begun. We anticipate seeing our first collisions with the Track Trigger in June, 2001. It will be important to measure the trigger rates as a function of luminosity as early as possible. These results will be compared to detailed extrapolations performed with Run I data.

7.3 The Effects of High Luminosity

Luminosity effects on Level 1 Track Trigger rates are spelled out in [4]. In that note, 3 distinct options (labeled scenarios A, B and C) were described in detail. The nominal starting point for Run IIa is option A. Options B and C call for higher momentum thresholds at higher luminosity. While these higher thresholds can keep the trigger cross section under control, the efficiency for the signal modes are reduced. For example, in going from option A to option C, the efficiencies for $B^0 \to \pi^+\pi^-$ and $B_s^0 \to D_s(n\pi)$ are all reduced by roughly a factor of two.

Our goal for the Run IIb Track Trigger would be first to recover the lost efficiency at higher luminosity without increasing the trigger cross section. We believe that we can do better than that, however, by both reducing the trigger cross section and improving the efficiency for the modes of interest. For example, if we were able to control the Level 1 cross section to the point where we could allow for 1.5 GeV/c tracks (current threshold is 2 GeV/c) we could significantly improve the efficiency for hadronic B decays.

[2]The Track Trigger sends 16 trigger bits to preFred. We reserve 1 of those bits to signify > 6 tracks and 1 bit to signify a bunch-0 crossing. This leaves 14 independent triggers that can be generated.

7.4 Track Trigger Upgrades

As stated above, the ongoing challenge for the all-hadronic B decay triggers will be the rate at Level 1. Therefore, the Track Trigger system will play a crucial role in our ultimate physics potential. If trigger rates are unacceptably high, then prescales will have to be implemented which reduce the size of the acquired signal samples. With good signal-to-noise, we will be able to implement more trigger configurations and access more decay modes with a higher efficiency.

The original Track Trigger design was aimed specifically at the physics of the two-body B hadron decays, such as $B^0 \to \pi^+\pi^-$. Since that time, the emphasis has shifted towards other hadronic modes, for example:

- B_s decays, such as: $B_s \to D_s\pi$ and $D_s 3\pi$, with $D_s \to \phi\pi^+$, K^*K^+, $K^0_S K^+$ for B_s mixing and CP violation measurements.
- $B^+ \to D^0 K^+$, with $D^0 \to K^+\pi^-$ or $K^+\pi^-\pi^+\pi^-$ for a measure of the angle γ.

These decay modes have higher charged multiplicities and therefore different kinematics than do the two-body modes.

Here we propose two potential upgrades to the Track Trigger. Although it is conceivable that both upgrades be implemented simultaneously, we present them here as two distinct improvements to the Track Trigger system.

The current version of the Track Trigger looks the axial tracking information (p_T, ϕ) of pairs of tracks. The first of the two upgrades we would like to consider is to expand the Track Trigger to look at triplets of tracks, the Three Track Trigger. The second of the two upgrades is to incorporate stereo tracking information into the Track Trigger, the Track Trigger 3D.

7.4.1 Three Track Trigger

Looking at triplets of tracks would be especially useful in designing hadronic B_s triggers, such as $B_s \to D_s^-\pi^+$, where $D_s^- \to \phi\pi^-$ and $\phi \to K^+K^-$.

Due to the three-track combinatorics, this upgrade will require additional lookup tables beyond those required for track-pairs. The current generation of static RAM devices are not large enough to handle these tasks. However, memory technology is improving quite rapidly. There is also the possibility of using dynamic RAM, which does currently exist in sizes large enough for this task.

Design of the Three Track Trigger will be an extension of the design of the Track Trigger. The memory issue will be a trade-off between the volatility of dynamic RAM and the sheer scope of the amount of static RAM necessary for the Three Track Trigger. If dynamic RAM is chosen, then we will need a mechanism for refreshing the contents of the RAM periodically. This could be achieved in normal operation during the Tevatron abort gaps, which are periods of empty crossings necessary for the machine to be able to dump the beams.

The Track Trigger can currently handle up to 15 different Level 1 triggers (14 two-track triggers plus 1 auto-accept for $\geq$6 tracks. This flexibility would be maintained in the upgrade, so that it would be possible to trigger on two-track combinations. In this scenario, for example, we might have the following triggers:

- two-track with low thresholds
- two-track with high thresholds
- three-track with low thresholds
- three-track with high thresholds

all with potentially different prescale factors. The $B^0 \to \pi^+\pi^-$ acceptance would remain, but we would have the ability to design improved triggers for higher multiplicity decays, such as the B_s modes listed earlier.

The Three Track Trigger would be a straightforward replacement to the Two Track Trigger. No other changes to the CDF trigger would be required.

7.4.2 Track Trigger 3D

The XFT uses only axial information from the COT, so it is not possible to calculate the invariant mass of track-pairs. A proposal to upgrade the XFT to include stereo tracking information exists [5]. Much of the infrastructure to implement stereo segment finding in the XFT has already been installed. To take advantage of this in the Level 1 trigger, the Track Trigger would need to be upgraded so that invariant mass criteria could be imposed on track combinations. Since the stereo segment information would come from the XFT on a path independent of the axial track information, the Track Trigger 3D would need to do the stereo segment matching in addition to the invariant mass calculation. Even a coarse measurement of the track stereo angles could greatly reduce the track trigger rate and open up significant new opportunities.

The currently proposed XFT upgrade matches axial tracks to stereo segments at Level 2. This is of no use to the Track Trigger. Here, we propose to bring the stereo segments over to the Track Trigger and do the matching at Level 1 for the Track Trigger only. In other words, stereo tracking information would not be available for Level 1 electrons or muons, only for the Track Trigger. This may be possible by using the latency in the XFT linker plus the XTRP.

The XFT stereo finders will find segments in parallel with the axial finders. After stereo segments are found, they could be sparsified and shipped directly to the Track Trigger. This would take place while the axial linkers were finding tracks and sending them out to the XTRP. The XTRP would then provide the list of axial tracks to the Track Trigger, while the stereo information is already in-hand. A look-up stage would then associate the axial tracks to stereo segments, then the Track Trigger could proceed with "3D" tracking information.

As a result of the initial version of this proposal, a proposal to perform axial-stereo track linking for all XFT tracks has been proposed [6].

7.5 Rate Considerations

We have looked at Run I data using an XFT + Track Trigger simulation. With Run I minimum bias data, we can look at the fraction of events that pass the trigger requirements and then normalize the trigger cross section to the absolute rates expected for the Run IIa Track Trigger [4]. From this information, we calculate the Level 1 accept rate relative to the "standard" scenario-A two track cuts. The scenario-A cuts are:

- each track $p_T > 2\,\mathrm{GeV/c}$
- $p_T(1) + p_T(2) > 5.5\,\mathrm{GeV/c}$
- opposite charge
- $\delta\phi < 135^\circ$, where $\delta\phi$ is the opening angle between the two tracks.

These cuts have been determined to be optimally efficient to accept both the two-body and three-body B decay modes. The Run IA Track Trigger will use these selection criteria.

7.5.1 Three Track Trigger

Using the Run I data, we can investigate the effect of adding a third track into the event selection. As stated previously, this will be of use for the B_s decay modes.

As an example, we have implemented the following three track cuts:

- each track $p_T > 2\,\mathrm{GeV/c}$
- two tracks of opposite charge
- $\delta\phi_{min} < 22.5^\circ$
- $\delta\phi_{max} < 60^\circ$

where $\delta\phi_{min}(\delta\phi_{max})$ is the minimum(maximum) opening angle between two tracks. Notice we have dropped any momentum cut on the sum of the track momenta.

The results as a function of luminosity are shown in Figure 19. The luminosity is shown for 132 ns running, where we are using Run I data to map out the cross section as a function of luminosity. The points shown are data, not an extrapolation. As can be seen from the plot, the statistics are limited at high luminosity.

The trend is clear. The scenario-A cross section is rising quadratically with luminosity. The three track cross section is significantly lower than the two-track cross section and also grows more slowly with luminosity.

This trigger would pick-up multibody B decays, but it would not catch two-body decays. Another set of targeted two body cuts could be used in conjunction with the three-track cuts shown.

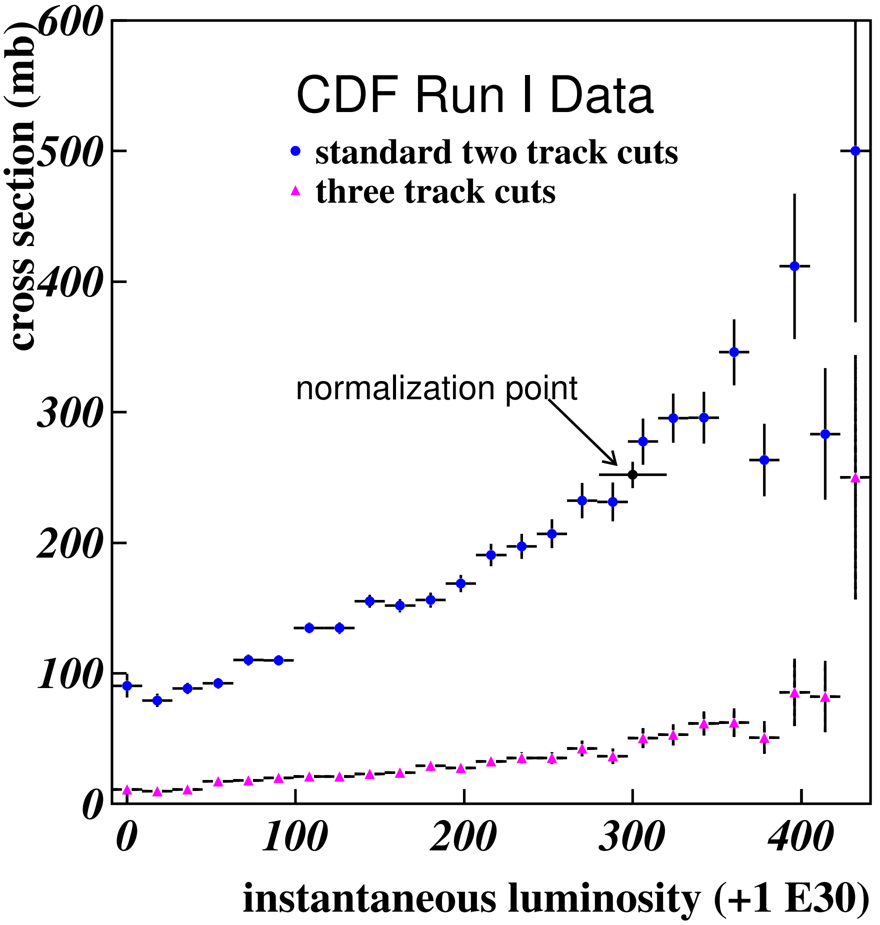

Figure 19: Trigger cross section as a function of luminosity for 132 ns bunch spacing. The points are Run I data where we have simulated the XFT and Three Track Trigger. The rate reduction over the Run IIa Track Trigger scenario-A cuts is significant.

We have not yet attempted to optimize these cuts, nor have we evaluated the effect of these cuts on efficiency for the signal. It is clear, however, that the additional handles provided by the Three Track Trigger will provide the opportunity to continue to trigger on hadronic B decays even at very high luminosity.

7.5.2 Track Trigger 3D

To simulate the Track Trigger 3D, we additionally used the XFT3D simulation to properly account for the invariant mass resolution of the track-trigger.

Including stereo information at Level 1 and simply add an additional mass window cut:

- $4.75\,\mathrm{GeV} < m_{12} < 5.75\,\mathrm{GeV}$

to the scenario-A trigger requirements, we can significantly reduce the trigger cross section.

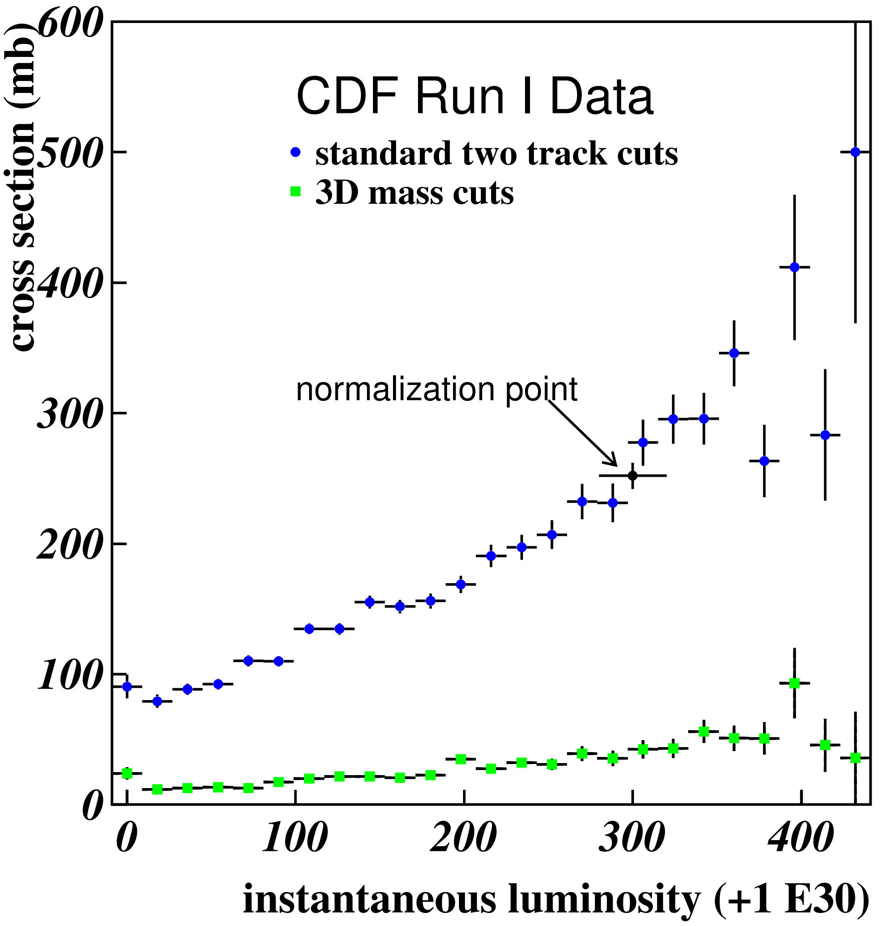

Figure 20: Trigger cross section as a function of luminosity for 132 ns bunch spacing. The points are Run I data where we have simulated the XFT and Track Trigger 3D including stereo information. The rate reduction over the Run IIa Track Trigger scenario-A cuts is significant.

The result is shown in Figure 20. The rate is calculated by looking at the number of minimum bias events passing the trigger requirements **relative** to the "standard" scenario-A cuts implemented with the Run IA Two Track Trigger. The reduction in cross section is significant. For example at a luminosity of $3 \times 10^{32}\,\mathrm{cm}^{-2}\mathrm{s}^{-1}$, the scenario-A cross section is $450\,\mu$b (a rate of $180\,k$Hz), while the Track Trigger 3D cross section is about $80\,\mu$b (a rate of $32\,k$Hz.) Even a rate of $32\,k$Hz rate is too high for the two body B decay modes, but only minimal additional cuts would be necessary to acheive an acceptable rate. In the case of the Run IA Two Track Trigger, the additional momentum cuts required to achieve an acceptable Level 1 rate would be so severe that virtually all efficiency for the signal would be lost.

Although the lower set of points in Figure 19 and Figure 20 look similar to one another, the two curves are arising from different sets of requirements. There are a significant number of events common to the samples, primarily arising through the $N_{track} > 6$ auto-accept condition. This is discussed further in the next section.

For the Track Trigger 3D, Figure 20 is not the full story. A straight invariant mass cut around the B mass would reject a large fraction of the multibody B decays that we would like to accept.[3] But this is still a net winner, because we would have an additional handle and more available bandwidth to accept the multibody decays.

7.5.3 Other Considerations

It is also worth noting that one of the ultimate limitations in rate reduction for a track-based trigger is the multiplicity constraint. With the track trigger, we automatically issue a Level 1 accept if there are more than 6 tracks with $p_T > 2\,\mathrm{GeV/c}$. There are two reasons for this:

1. The combinatorics for higher multiplicity events makes processing within the limited Level 1 time impractical.
2. A large fraction of the higher multiplicity events would satisfy the two-track requirements anyway.

For the standard two-track cuts, 10-15% of the accepted events are due to $N_{track} > 6$. So far, we have not considered altering this requirement. If the N_{track} requirement is maintained, then the absolute boundary for track trigger rate reduction would be a factor of 7-10, where the only remaining events coming in on the N_{track} requirement. This is extreme, of course, because a reduction of that magnitude would, by definition, throw out a lot of signal as well. To achieve further track-trigger rate reductions would require revisiting the N_{track} cutoff. Although we are not proposing that change at this point, we are also not totally rejecting that option, either.

Further studies are necessary to fully understand how to optimally implement the mass cut in the trigger. For example, how do we handle tracks without a stereo segment? How does the rate behave with a p_T cut of $1.5\,\mathrm{GeV/c}$ on the two tracks? What complementary triggers become available?

As an example of possible new triggers we can consider, we have started looking at the rates for a dedicated Level 1 $\phi \rightarrow K^+K^-$ trigger. The trigger would be followed by an SVT requirement at Level 2. A dedicated ϕ trigger would provide large samples of B_s decays. Preliminary studies indicate that the Level 1 rates when a 3D mass cut is included are quite manageable.

7.6 Plans/Outlook

Before embarking on these upgrade paths, it is crucial to take colliding beam data and gain experience with the first generation of the Track Trigger. Once this happens, it is quite likely

[3] The multibody decays would be ideally addressed with the 3-track trigger option.

that we will very quickly learn how to drastically improve the trigger system and open up new avenues for hadronic B decays. After all, 25% reduction in track-trigger rate is worth $\sim 8k$Hz at Level-1, which is roughly 20% of **all** available Level-1 bandwidth!

The layout and fabrication of the Two-Track Trigger proceeded rather quickly thanks to the experience gained designing, constructing and debugging the XTRP data boards. Working from an existing Two-Track design, we anticipate that an upgraded Track Trigger system could be designed, built and implemented in a relatively short time scale.

Of the upgrades listed above, the Three-Track Trigger is more straightforward than the Track Trigger 3D. The implementation of the trigger look-ups is similar in both cases, but the Track Trigger 3D requires the two additional steps of producing a sparsified list of stereo segments and axial track matching.

7.7 Conclusion

The Two-Track Trigger will be operational at the beginning of Run IIa. Based upon our experience and physics goals, we feel it will be very beneficial to construct a second generation Track Trigger system to further exploit the physics potential of CDF.

References

[1] S. Donati and G. Punzi, CDFNOTE 3167 (1995).

[2] S. Donati and G. Punzi, CDFNOTE 3780 (1996/1999).

[3] J. Mueller and P. Wilson, CDFNOTE 2665 (1994).

[4] I. Yu and J. Lewis CDFNOTE 4095 (1997).

[5] J. Hoftiezer *et al.* CDFNOTE 4300 (1997).

[6] R. Hughes *et al.* "Expression of Interest: Adding Stereo Segment Finding and 3D XFT Tracking in the Trigger for Run IIb."

8 Data Acquisition Upgrades

8.1 Introduction

For this discussion Data Acquisition (DAQ) refers to hardware and software used to readout the front end electronics and transport the data to the VME Readout Buffers (VRBs) from which the Event Builder reads out the data fragments. The data logging computers and disks located in B0 and the control room computers and monitors are also considered part of the DAQ.

For Run IIa we are expected to handle a sustained rate of 300 Hz into Level 3 with events sizes on average of 250KB. For Run IIb we should be able to handle rates of 1000 Hz with similar event sizes. Upgrades to the detector and higher luminosity conditions may result in larger event sizes.

Although the Level 1 trigger system for CDF is essentially deadtimeless, the performance of the Level 2 trigger and the DAQ system together will largely determine the overall system livetime. The ability to support a rate of 1000 Hz being sent to the Event Builder with good ($> 85\%$) livetime depends upon maintaining a Level 1 trigger rate of < 45 kHz into an asynchronous 4-deep event buffer upon which the Level 2 trigger system operates in a pipelined fashion, with 10 microsecs allocated each to gathering and processing the event.

8.2 Readout Performance

During commissioning we have seen readout limits attributed to several subsystems. These limits have more than one source, some of which we expect can be improved with more efficient software. Some sources of readout limits include: front end electronics processing time, data formatting by the VME Readout Controller and the event size. Improvements to the readout time include changing the mode of readout from single to block transfers, limiting the readout of non-critical monitoring banks and possible improvements to the underlying VME readout routines. Some subsystems require significant processing time in order to format the data. Once we gain some experience with the hardware we can also limit the data volume by performing zero suppression and possibly writing the data in a more compact format. In addition we can pursue more efficient front end readout routines by reading out an event while processing the previous event. To further improve readout performance it may be required to upgrade selected processors.

The long processing time of the TDC DSPs can be a potential problem. The processing time is dependent on the number of hits that the TDC must digitize which is currently set to a maximum of 8 hits. We have seen cases where one TDC with many noise hits can slow down the rate. We do not have much experience with high occupancy in the COT under different operating conditions which may also lead to a slow readout rate. Although the average processing times of the TDCs can be reasonable, the throughput rate is dominated by the tails in the distributions of the processing time and having just one TDC that takes a lot of time can have a significant impact on the rate. We had hoped to gain some experience under realistic operating conditions during the first 36×36 store, however the run was ended sooner than expected and we were unable to complete our tests. The long processing times may be controlled by limiting the maximum number of hits and once we gain some experience we may pursue this option.

We do not expect a major upgrade to the DAQ, however we will not know the limitations of the system until we have some experience running under realistic conditions. Although it is anticipated that the required performance can be achieved with the existing hardware, it would be useful to evaluate the compatibility of newer processors in a teststand and pursue optimizations to the readout code.

8.3 Level 2 Decision

We will need operational experience with the Level 2 trigger system in order to fully understand its performance and identify any limitations and bottelnecks. This system is just now being commissioned. Possible improvements may include upgrading the processors (the current processors were built in 1998) and bringing more data into the the Level 2 system, such as the stereo information from COT layer discussed previously.

8.4 Software Updates

We depend on several non-Fermilab products: SmartSockets, Java, Linux, VxWorks, Oracle. We have to be careful when updating software to ensure that we have compatible versions of the different packages. The message passing system relies on the commercial package SmartSockets and is a critical element of the DAQ. If we upgrade the front end processors/operating system we may run into compatibility problems. We had paid the vendor to port the software to run under VxWorks in the VME Readout Controllers. Although we do not have plans to port the software to newer platforms we may be forced to if we have a need for faster VME readout controllers and they are not compatible with the version of VxWorks we are using. Additional components or monitoring tasks may require that we buy more SmartSockets licenses or pay for porting the software to new platforms and/or operating systems.

8.5 Computing Infrastructure

The online system currently maintains approximately 50 Linux PCs, 7 mid range file servers for code development and data logging and a couple WindowsNT based PCs. We anticipate having to replace aging systems as needed and it is likely that parts of this system as well as the network connection with have to be updated during Run II.

```
Maintanance Cost

20 PCs              50K
File Server        100K
Networking     50-100K
Misc                50K
Software           100K
----------------------
Total         350-400K
```

8.6 New Readout/Hardware

It would be vastly preferable for any additional detectors or upgrades for Run IIb to fit in within the existing DAQ framework with formatted detector data being sent to the VRBs. Client have to communicate with the run control so the platform should be compatible with the message passing software. The addition of new hardware would require personal to write software and integrate the component.

9 Event-Builder and Level 3 PC Farm

9.1 Introduction

In this section we discuss the expect needs and strategies for upgrading the Event-Builder and Level 3 PC farm. For the Technical Design Report of the CDF II detector, the Level 2 trigger provides an accept rate of 300 Hz corresponding to an input rate into the Event-Builder and Level 3 farm of about 75 MBytes/s assuming an event size of 250 kBytes. This design goal is based on a peak luminosity of $2 \cdot 10^{32}\text{cm}^{-2}\text{s}^{-1}$. According to the Tevatron upgrade plans a maximum peak luminosity of roughly $5 \cdot 10^{32}\text{cm}^{-2}\text{s}^{-1}$ is reached by 2006. Naive scaling predicts a Level 2 accept rate of at least 750 Hz.

However, the Event-Builder data throughput depends not only on the Level 2 accept rate but also on the event size which is closely related to the detector occupancy. The CDF silicon detectors provide the single largest part of the event data and their occupancies depend on the threshold requirements and the signal to noise ratio. Ideally the occupancy is smaller than 5 % which corresponds to 750,000 channels $\times$ 0.05 $\times$ 2 Bytes = 75 kBytes per event. Due to radiation damage the signal to noise ratio is expected to decrease during the Run II data taking, and depending on the threshold tuning, the occupancy might change. To allow for useful pattern recognition, the occupancy should not exceed 10 %, corresponding to 150 kBytes per event. This increases the total event size of about 250 kBytes to 325 kBytes. To account for these types of effects a factor of two on top of the original 250 kBytes event size is applied as a safety margin. This implies a bandwidth of 500 kBytes $\cdot$ 750 Hz = 366 MBytes/s for the Event-Builder for Run IIb.

The maximum bandwidth theoretically achievable with the existing Run II system is 15 channels $\times$16 MBytes/s = 240 MBytes/s. In practice about 60 % of the theoretical limit has been achieved in benchmarking tests with simulated data sizes corresponding to the expected detector occupancy. It is likely that the performance under test conditions can be further improved to about 80 % of the theoretical limit after tuning the system. The performance when processing real data depends crucially on the load balancing among the various ATM switch inputs.

To be conservative, two different Run IIb options are described, ranging from the minimum of simple maintenance of the existing system, to an upgraded system capable of sustaining a bandwidth of at least 400 MBytes/s.

Estimating the CPU power needs in the Level 3 Trigger PC farm is more uncertain than estimating the bandwidth needs for the Event-Builder. For the Level 3 PC farm the achievable performance increase per PC is discussed.

This project is being pursued by the MIT group: K. Anikeev, G. Bauer, A. Bolshov, J. Friedman, I. Furic, B. Iyutin, A. Korn, I. Kravchenko, N. Leonardo, M. Mulhearn, S. Rakitin, Ch. Paus, L. Rosenson, K. Sumorok, S. Tether, J. Tseng, and F. Wuerthwein.

9.2 Limitations of the Existing System

The typical Event-Builder and Level 3 PC farm setup is shown in Figure 21. In Figure 21 only three processor nodes per subfarm are depicted while this number is actually four to five times larger for the Run II startup. When analyzing the CDF Event-Builder and Level 3 PC farm, two different types of limitations can be identified: *throughput limitations* and *processing power limitations*. Processing power limitations can in principle be overcome; computing power is made available by purchasing CPUs. Hopefully the Level 3 trigger algorithms can be adjusted to perform with the available CPU and still preserve the desired physics.

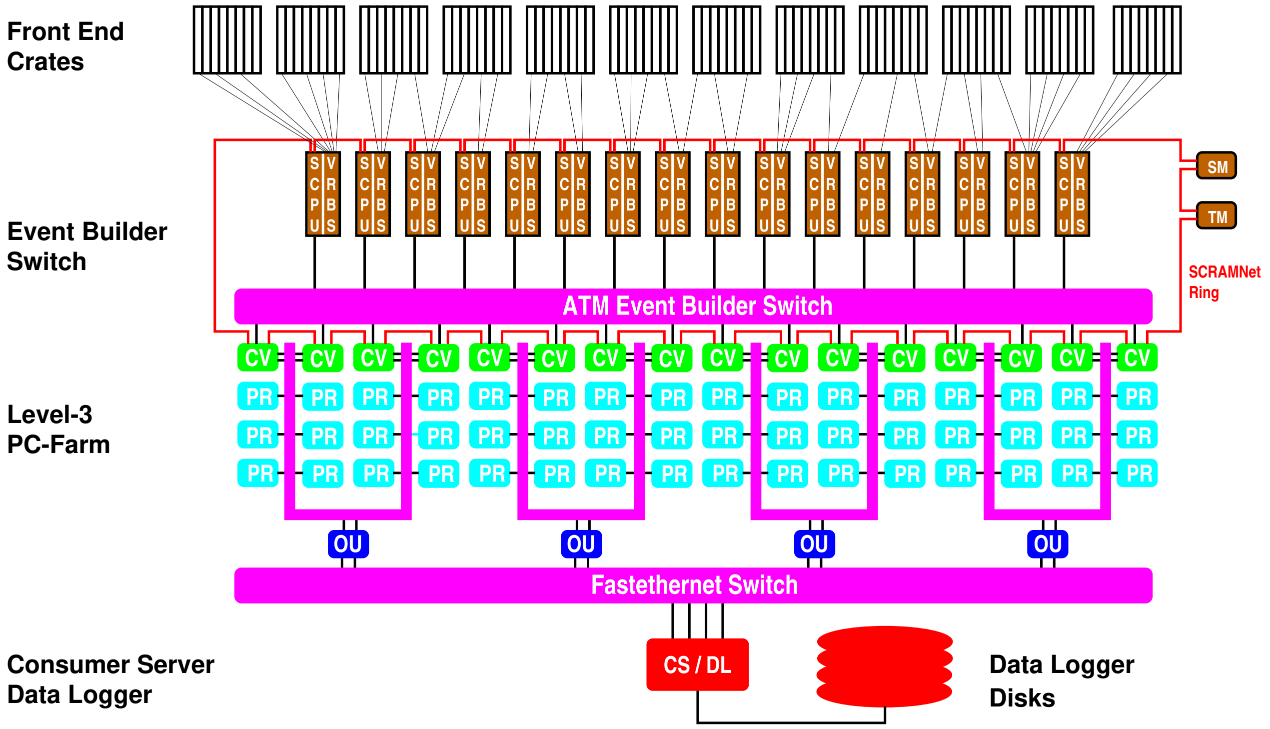

Figure 21: Event-Builder and Level 3 PC Farm setup for Run IIa.

Zooming in on the typical Event-Builder and Level 3 PC farm setup as shown in Figure 22, several possible throughput limitations are distinguished:

1. control network performance of the Event-Builder (rate limit)
2. at the Event-Builder input (VRB crate)
3. at the PC farm entry which are the converter nodes
4. internally in the processing farm; fast ethernet
5. at the Level 3 output to the Consumer Server and Data Logger (CS/DL)

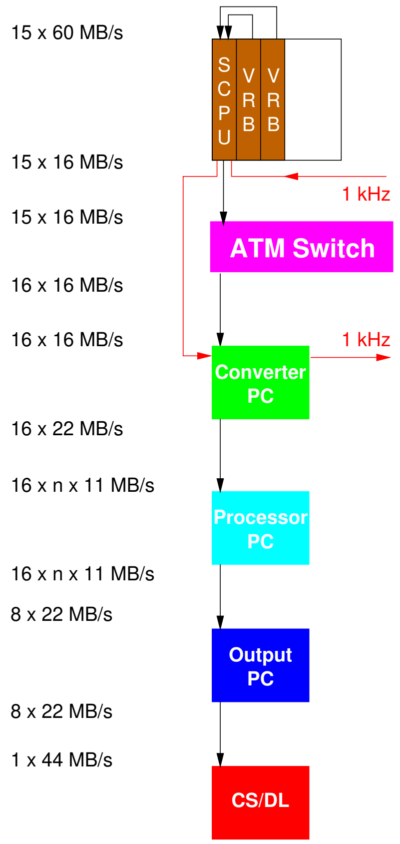

Figure 22: Event-Builder and Level 3 PC Farm: scheme of possible throughput limitations.

The Event-Builder limitations for the data throughput are about 240 MBytes/s given by the 15 ATM input connections (OC3 standard). With event sizes of 250 kBytes the control network therefore has to function properly up to 1 kHz, and this performance has been demonstrated.

Both, 240 MBytes/s data throughput and 1 kHz event rate, are upper limitations and the real performance will be less, depending on parameters such as the load balancing per ATM input, the fluctuations of the event fragment length and so on. With the present experience a sustained rate of 600-800 Hz of 250 kBytes events should be achievable without further extensions.

The input into the Level 3 PC farm on the other hand is less problematic since there is one more output OC3 connection for a total of 16. The fact that the converter node cointains many PCI cards, i.e. SCRAMNet, ATM, quadruple fast ethernet, has so far not caused any problem. The two fast ethernet output connections have a sustained rate through the converter node of more than 20 MBytes/s while the OC3 input connection provides 16 MBytes/s maximum input.

For the subfarm internal network the maximum rate of 16 MBytes/s is subdivided to at least 8 PCs which is a comfortable rate for a 24 port fast ethernet switch.

Without rejection one output node, with 2 fast ethernet connections to the subfarm and 2 fast ethernet connections to the switch which connects to the Consumer Server and Data Logger, is able to handle one complete subfarm. Assuming a reasonable event rejection rate an output node could handle the input of more than 2 subfarms on its own. No limitations are expected in that layer. Extension to include more PCs is trivial since fast ethernet switches serving up to 64 ports exist on the market. Concerning the CS/DL side the Level 3 PC farm, software has been designed to communicate with a farm implementation of this device. The extension is trivial and hardware can be bought off-the-shelf.

9.3 Event-Builder Upgrade Scenarios

In this section two upgrade scenarios are described, one of which is simply to maintain the status quo which should be able to handle a sustained data throughput of roughly 200 MBytes/s and a maximum rate of 800 Hz. The proposed upgrade scenarios are based on the assumption that in general the CDF data aquisition will not exceed a sustained data throughput of 400 MBytes/s and a maximum rate of 1.5 kHz. For each upgrade scenario, both the human resource needs, as well as the equipment costs are discussed.

Upgrade scenarios replacing the ATM switch technology completely using for example Gigabit Ethernet or MyriNet are not considered because they require significanly more work and are not seen as being necessary at this stage.

9.3.1 Maintaining the Status Quo

As discussed above, the existing system is likely to sustain a Level 2 accept rate of $600-800$ Hz for an event size of 250 kBytes. To maintain this level of performance until 2008 requires to plan for hardware failures. Some of the hardware as well as some software will be obsolete and thus no longer commercially available.

In the following the hardware of the Event-Builder is listed and issues of obsolescence and potential replacement needs are discussed.

- The ATM cards in the SCPU crates are already obsolete. Enough spares have been purchased to be prepared for a long run.
- ATM cards in the Linux PCs are currently going out of production. This process is being watched closely and sufficient spares will be purchased.
- The ASX 1000 ATM switch has a huge installed base and the vendor, Marconi, guarantees that they will back this product indefinitely.
- In Run I SCRAMNet was used for the control network was very stable after the initial shakedone. Some more spares have to be bought to extend the system for Run IIb.
- The scanner CPUs are commercial MVME 2600 single board computers with a large installed base. They will be available until the beginning of Run IIb and depending on the failure rate more modules may have to be purchased.

The main worry of the software is the ATM driver on the Linux PCs. The operating system on the converter nodes is already running an older version in order to be able to use the driver which had to be significantly changed from its original version. It is expected that the operating system on the farm will need to be updated at least once or twice and it might be necessary to adapt the driver to the newest Linux release.

Between now and 2008 roughly \$100K are needed for spare parts, and at least one FTE year on software development to maintain the system at 600-800 Hz Level 2 accept rate at 250 kBytes event size.

9.3.2 Upgrading the ATM Network

The natural upgrade path for Run IIb is to switch from the present OC3 to OC12 ATM links and buy something like the new switch ASX 4000 from Marconi. Switch ports based on the OC12 standard provide 4 times the bandwidth of the corresponding OC3 ports corresponding to a theoretical limit of close to 1000 MBytes/s, $60-80\%$ of which ought to be achievable in practice if there were no other bottlenecks.

The system limitations are then likely to be not the ATM switch but instead:

- VRB readout bandwidth via VME: 1000 MBytes/s spread evenly over 15 VME crates results in a 67 MBytes/s bandwidth requirement within each VME crate. This can not be achieved with present VME hardware and protocols. Benchmarks of the D64 read/write bandwidth for a MVME2600 came close to 50 MBytes/s. The useful bandwidth is probably as low as 30-40 MBytes/s resulting in 450-600 MBytes/s sustained throughput rate for the Event-Builder. This rate exceeds the maximum required performance of 400 MBytes/s and a maximum rate of 1.5 kHz as discussed above.

- The present system is limited to about 1 kHz Level 2 accept rate due to the maximum message passing rate over the SCRAMNet ring. This limitation is not due to the hardware but the software. To go beyond this the message passing protocol needs to be upgraded.
- The Converter nodes presently feed their subfarms via two fast ethernet links on a 4 port card. The output bandwidth can be doubled by making use of all four ports without additional hardware. The total bandwidth through the converter nodes is then up to 48 MBytes/s which matches the performance of the ATM connection.

A sustained Event-Builder bandwidth of $450 - 600$ MBytes/s is achievable in this scenario. Past experience has shown that in the Event-Builder the usage of the ATM switch is sufficiently different from its commercial use in the telephone industry. This implies that commercially available drivers have to be modified in a non-trivial way. This is expected to be the largest software development effort in this scenario.

The cost of the upgrade including the new switch and all necessary network interface cards is estimated to be \$500K but should be re-evaluated in the future.

The total software development for the two ATM drivers, plus changes to the SCRAMNet message passing protocol are estimated to amount to $2 - 3$ FTE years.

9.4 Level 3 PC Farm Upgrade

At present it is too early to provide reliable estimates of the CPU needs for the Level 3 PC farm over the course of Run IIb. Instead it is pointed out that the performance/price ratio has roughly doubled every 1.5 years in the past. A replacement of the obsolete PCs in 2004 will therefore probabaly quadruple the present processing power. A total budget of about \$500K is proposed for a Level 3 PC farm upgrade. Roughly \$350K are needed to replace hardware that will be obsolete at that point and another \$150K are proposed to further increase the processing power.

9.5 Conclusions

To adjust the Event-Builder and the Level 3 PC Farm to the needs of the upcoming Run IIb an extension of the data throughput to upto 366 MBytes/s and a maximum rate of 1.5 kHz are envisaged.

For the Event-Builder, maintenance of the present system can deal with up to 200 MBytes/s and 800 Hz at a cost of about \$100K. For higher performances a straightforward extension of the ATM switch from OC3 to OC12 optical fibers is forseen at a cost of roughly \$500K.

The Level 3 requirements for Run IIb are less well defined at this stage. It seems that a replacement of the in 2004 obsolete PCs with the same number of PCs and a further extension by roughly half of that system should cover the needs of the experiment. This will require roughly \$350K for pure mentainance and another \$150K for the further extension of the CPU power.

In summary the minimal cost to maintain the present setup is \$450K and the maximal necessary extension is \$1M. There are no explicit contingencies in these numbers.

10 Estimated Costs for Upgrades (Excluding Silicon Tracker Replacement and Offline)

In the following table we list the estimate costs, not including labor or contigency, for the anticipated upgrades of the detector, trigger and online data acquisition system.

Project	Cost	R&D 2001	R&D 2002
Projective COT	$150K		
Central Preradiator	$425K	$20K	$30K
Timing for EM Calorimeters	$275K		
CSX Scintillator Replacement	$150K		
Inclusion of Stereo in XFT	$170K	$15K	
Track–Trigger	$160K		
DAQ/Online	$500K		
HEVB and L3 Trigger	$1000K		
Total	$2830K	$35K	$30K

Table 3: The estimated costs for upgrades

11 CDF Run IIb Upgrade Steering Committee

The members are:
Gerry Bauer (MIT), Giorgio Chiarelli (Pisa), Frank Chlebana (FNAL), Henry Frisch (Chicago), Michael Lindgren (UCLA), Pat Lukens (FNAL), Takashi Ohsugi (Hiroshima), Luciano Ristori (Pisa), Michael Schmidt (chair, Yale), Jeff Spalding (FNAL) and Avi Yagil (FNAL).

11.1 Recommendations for Run IIb Upgrades (excerpts)

The Run IIb Steering Committee was formed to solicit, collect and review proprosals from the collaboration for upgrades to CDF for Run IIb, defined roughly as the period after 2 fb^{-1} of data is collected. The charge to the committee from the spokespersons and the laboratory was to evaluate and prioritize these proposals according to their feasibility and relevance for maintaining the capabilities of CDF for Run IIa into Run IIb.

Proposals explicitly reviewed by the committee include (working from the inside–out):

- SVXII/L00 replacement (silicon strips and pixel options)
- 'Projective' COT
- Scintillator upgrade of Central Preshower Radiator
- Including timing information from CEM and PEM
- Replacement options for aging CSX scintillation counters
- Adding stereo information to the XFT trigger
- Track–trigger upgrades
- Upgrades and maintenance of the online DAQ system
- Upgrades and maintenance of the Hardware Event Builder and Level 3 trigger farm

11.2 Recommendations on SVXII/L00 Replacement:

1. Of all the upgrades considered by CDF for Run IIb, the replacement of the SVXII/L00 has the highest priority. The loss of the inner layers of the silicon tracker due to radiation damage would compromise almost all aspects of the CDF research program. While it is difficult to know with great precision at what integrated luminosity the SVXII/L00 replacement will be necessary, we need to prepare for the case that the value turns out to be not much more than a few inverse fb.

   The CDF Run IIb Upgrade Steering committee was guided by results of the Silicon Working Group (see `http://ncdf12.fnal.gov/PAC/pac_april_01.html` for the proposal submitted to the PAC in November 2000). The full replacement of SVXII/L00 using single-sided sensors readout by the SVX4 chip is considered a CRITCAL CDF upgrade for Run IIb. The scale of the project is such that we can not wait until sufficient data and dosage is accumulated in Run IIa to sharpen our predictions for when the performance of the current detectors will be severely compromised.

2. The design of the silicon strip replacement for SVXII/L00 should be driven by two criteria:

   a. The performance should be at least equal to that expected from SVXII/L00 working together with ISL and COT.

   b. To the extent that criteria a. is fulfilled, design choices should favor the simpler design, where it is assumed that the simpler design is the one that increases the probability of being able to meet the schedule for the replacement in 2004.

3. Pixel options should be dropped. The primary and overriding reason for this decision is the steering committee's concern of the overall risk for CDF to keep to the aggressive schedule required to meet our own goals of replacing SVXII/L00 during a six month shutdown beginning in July of 2004.

11.3 Recommendations on Other Upgrades

CDF will be in a better position to sharpen the arguments and make detailed designs for many of the other Run IIb upgrades once sufficient data is collected and analyzed from the completed Run IIa detector. The geometry of the detector and material distribution has been substantially changed from Run I and this is likely to affect the hit multiplicities observed in many of the detector subsystems. This can have important implications for what threshold levels are required to control trigger rates, the size of events and ultimately the number of events that can be taken to address specific physics topics. The performance of the detector subsystems can also be effected (e.g. electron identification). These and other effects are most reliably determined and intepreted from analyses of data.

In some cases it we may find that it is highly desirable to install a particular upgrade in advance of the shutdown required for the SVXII/L00 replacement or that it may be possible to stage a particular upgrade for installation after Run IIb is underway.

Keeping these comments in mind we turn to the recommendations for the other Run IIb upgrades:

1. The committee recommends that R&D efforts for the 'projective' COT upgrade be pursued. Extrapolations from past performance of the inner layers of the CTC during Run Ib suggest that the 'projective COT' upgrade is likely to be ESSENTIAL for CDF during Run IIb. The dependence of almost all analyses on the tracking system argues for giving high priority consideration for this upgrade. The decision to proceed with installing this upgrade should be based on:

   a. The results of R&D for a suitable method of deadening the sense wires at large z

b. Thorough evaluation and review of the risks of the upgrade for the COT

c. Thorough understanding of the how the 'projective' COT will preserve the performance of the full CDF tracking detector system (COT, ISL and upgraded SVXII/L00) into Run IIb. This should be based on an appropriate mix of studies based on Monte Carlo and Run IIa data (e.g. mixed events)

d. A thorough understanding of the schedule required for installation and checkout

2. The committee recommends that R&D efforts for the CPR2 upgrade be pursued. The scintillator based upgrade to the Central Preshower Radiator is well motivated. Many key analyses depend on the ability to identify electrons or separate single photons from meson backgrounds. It will be ESSENTIAL to replace the present wire chamber detectors which will become useless once collider operations with 132 nsec bunch structure (otherwise) becomes the norm for data collection. The decision to proceed with installing this upgrade should be based on:

   a. The results of R&D leading to a suitable design which minimizes cost while achieving sufficient performance

   b. A thorough understanding of the expected performance of the upgraded detector (through simulations and studies of data, including from Run IIa)

3. The committee recommends that R&D efforts for the CEM/PEM timing upgrade be pursued. The benefit of having the additional handle of timing information to reduce cosmic ray backgrounds and confirm that photons in unusual events makes this a DESIRABLE upgrade. The decision to proceed with installing this upgrade should be based on:

   a. The continued efforts to minimize the risk to the detector (e.g. CEM base modification strategy, in situ testing)

   b. The continued efforts to minimize the cost

4. CSX Replacement:

   a. The committee recommends a vigorous program to determine and monitor the efficiency of the CSX counters by any and all reasonable means. It is recognized that the CSX, like the CSP, scintillator has become yellowed and that continued loss of transparency could seriously compromise performance, making a replacement 'upgrade' ESSENTIAL. It is imperative that we get early and precise information on the performance of the counters. It is hoped that comparison with precise measurements made in 1998, and perhaps measurements from Run Ib data, will allow us to accurately determine the rate of deterioration.

   b. The committee recommends that CDF make preparations to replace the CSX scintillator and that the baseline design be one of replacement of scintillator with scintillator. Given that we do not expect to make any major changes to CSX until we are well into (or hopefully at the end of) Run IIa, it is important to factor in the inherrent disadvantage to changing things at all at that point, let alone adopting a new technology. The baseline design for the CSX upgrade needs to be one that maximizes the probability that it will work very shortly after installation.

c. As stated in the prior set of recommendations, detailed design considerations (e.g. replacing inner layer counters only but with phototubes on each end, etc.) are best carried out in light of information that will be gained early in Run IIa about the rates and character (timing, etc.) of the backgrounds in CSX. To this we should add that a detailed design will also depend on a careful evaluation of the mechanical aspects (i.e. loading of the arches, cable plant issues, etc.)

5. The committee recommends that stereo information be added to the XFT trigger. At this point it seems likely that being able to include this information at Level 2 will be ESSENTIAL. The hooks for this upgrade are in place and the implementation is an extension of the prior work on XFT.

   The additional capability of including this information for a mass trigger at Level 1 should be evaluated together with proposed upgrades to the track trigger. Such an upgrade could be VERY DESIRABLE and perhaps necessary for continuing CDF's B physics program with fully hadronic decays.

6. The committee recommends that R&D for upgrades to the track trigger be pursued. These upgrades could be VERY DESIRABLE and perhaps necessary for continuing CDF's B physics program with fully hadronic decays into Run IIb. The additional capability of imposing mass constraints on a track trigger at Level 1 should be evaluated together with the proposed upgrades to the XFT.

7. The committee recommends that CDF anticipate the necessity for continued maintenance and upgrades of the online DAQ system, the Hardware Event Builder and the Level 3 farm. The extent to which these upgrades will be ESSENTIAL depends in a nontrivial way on the performance of the detector, front-end electronics and trigger systems (and the performance of the accelerator). The limitations of the full system are not yet fully understood and can only be mapped out once we start reliably taking data.

11.4 Rank Listing of Other Upgrades

1. projective COT
2. stereo XFT (into L2)
3. CPR2
4. CSX (once the need is established)
5. online (beyond maintenance; includes front-end and baseline trigger systems)
6. EVB/L3 (beyond maintenance)

7. CEM/PEM timing
8. track trigger

This list reflects an attempt to integrate the following inputs:

- that high priority be given to upgrades that are most needed to extend the Run IIa capabilities of CDF into Run IIb
- our present understanding of the likelihood of the broad physics program being compromised without the upgrade
- how much of the program would be adversely affected without the upgrade
- the recognition that upgrades of elements within the collision hall are harder to stage
- the interdependence of one upgrade on another (*e.g.* not much point making big changes to the L3 farm if the online rate into the Event Builder is the bottleneck)
- the relative priority for high p_T searches

It can not be overstated how important it is to keep in mind that this list of upgrades and relative priorities is subject to change based on what we will learn from the early running in Run IIa. The level spacing in priority implied by actually writing down a rank ordered list is surely much smaller than the uncertainties given our present knowledge of the actual performance of CDF in Run IIa. In short, we reserve the right to change our minds in the future.